Mineralogical Magazine, October 2012, Vol. 76(5), pp. 1175–1207

The heteropolymolybdate family: structural relations, nomenclature scheme and new species

A. R. KAMPF[1,*], S. J. MILLS[2], M. S. RUMSEY[3], M. DINI[4], W. D. BIRCH[2], J. SPRATT[3], J. J. PLUTH[5], I. M. STEELE[5], R. A. JENKINS[6] AND W. W. PINCH[7]

[1] Mineral Sciences Department, Natural History Museum of Los Angeles County, 900 Exposition Boulevard, Los Angeles, California 90007, USA
[2] Geosciences, Museum Victoria, GPO Box 666, Melbourne, Victoria 3001, Australia
[3] Earth Sciences Department, Natural History Museum, Cromwell Road, London SW7 5BD, UK
[4] Pasaje San Agustin 4045, La Serena, Chile
[5] Department of the Geophysical Sciences, The University of Chicago, 5734 S. Ellis Avenue, Chicago, Illinois 60637, USA
[6] 4521 N. Via Madre, Tucson, Arizona 85749, USA
[7] 19 Stonebridge Lane, Pittsford, New York 14534, USA

[*Received 15 July 2012; Accepted 10 August 2012; Associate Editor: Frank Hawthorne*]

ABSTRACT

Type specimens of the molybdoarsenates betpakdalite, natrobetpakdalite and obradovicite and the molybdophosphates mendozavilite, paramendozavilite and melkovite, and similar material from other sources, have been examined in an effort to elucidate the relations among these phases, which we designate as the heteropolymolybdate family of minerals. Using electron microprobe analysis, X-ray powder diffraction and single-crystal X-ray diffraction with crystal structure determination where possible, it was found that natrobetpakdalite, mendozavilite and melkovite are isostructural with betpakdalite and that obradovicite has a closely related structure.

The betpakdalite and obradovicite structure types are based on frameworks containing four-member clusters of edge-sharing MoO_6 octahedra that link by sharing corners with other clusters, with $Fe^{3+}O_6$ octahedra and with PO_4 or AsO_4 tetrahedra (*T*). The structures differ in the linkages through the $Fe^{3+}O_6$ octahedra, which produce different but closely related framework configurations. The structures contain two types of non-framework cation sites, which are designated *A* and *B*. In general, there are two or more *A* sites partially occupied by disordered, generally larger cations that are coordinated to O atoms in the framework and to H_2O molecules. The *B* site is occupied by a smaller cation that is octahedrally coordinated to H_2O molecules. The general formula for minerals with either the betpakdalite or the obradovicite structure is: $[A_2(H_2O)_nB(H_2O)_6][Mo_8T_2Fe_3^{3+}O_{30+7}(OH)_{7-x}]$, where *x* is the total charge of the cations in the *A* and *B* sites (+3 to +7) and *n* is variable, ideally 17 for arsenates and 15 for phosphates. The ideal total number of *A* cations is defined as 2 in the general formula, but varies from 1 to 3.8 in analysed samples. Dominant cations at the *A* site include K, Na and Ca and at the *B* site Na, Ca, Mg, Cu and Fe. The combinations that have been identified in this study define six new heteropolymolybdate species.

A suffix-based nomenclature scheme is established for minerals of the betpakdalite, mendozavilite and obradovicite groups, with the following root names based on the structure types and the *T*-site cations: betpakdalite (*T* = As), mendozavilite (*T* = P) and obradovicite (*T* = As). Two suffixes of the form *-AB*, corresponding to the dominant cations in the two different types of non-framework cation

* E-mail: akampf@nhm.org
DOI: 10.1180/minmag.2012.076.5.09

sites complete the species name. The historical name melkovite is retained rather than introducing mendozavilite-CaCa.

Our investigation of the paramendozavilite type specimen revealed no paramendozavilite, but an apparently closely related new mineral; however, another sample of paramendozavilite analysed had K > Na.

Keywords: heteropolymolybdate family, crystal structure, new mineral, betpakdalite, melkovite, mendozavilite, obradovicite, paramendozavilite.

Introduction

In the course of research on a new Na- and Cu-dominant molybdophosphate from the Lomas Bayas mine, Antofagasta, Chile, the phase was determined to be essentially isostructural with betpakdalite. This led to a detailed study of other molybdophosphate and molybdoarsenate minerals in an effort to elucidate their interrelationships. The other species examined were natrobetpakdalite [sodium betpakdalite; renamed by Burke (2008)], melkovite, mendozavilite, paramendozavilite and obradovicite. For each of these species, type material was studied. We did not locate any specimens designated as holotypes; all were designated cotypes except the obradovicite specimen, which was simply designated as a type. In the course of the study we identified four new minerals with the betpakdalite structure type, two new minerals with the obradovicite structure type and one potentially new mineral which appears to be closely related to paramendozavilite.

Specimens from the collections of the Natural History Museum of Los Angeles County (prefixed NHMLAC), the Natural History Museum, London (prefixed BM), the Fersman Mineralogical Museum (prefixed FMM), the Colorado School of Mines (prefixed CSM), the Harvard Mineralogical Museum (prefixed HMM), the US National Museum of Natural History (Smithsonian Institution; prefixed NMNH), Museum Victoria and various private collectors have been used in the course of this study.

Unfortunately, these minerals are typically fine-grained and well formed crystals are commonly twinned. Nevertheless, we were able to obtain structure refinements for four species with the betpakdalite structure type, including type betpakdalite; to solve the structure of obradovicite; to refine the structures of two new obradovicite analogues; and to obtain unit-cell parameters for paramendozavilite. Comparative powder X-ray diffraction proved effective in demonstrating structural relationships and obtaining refined cell parameters for those species for which single crystal studies were not possible. Electron microprobe analyses were obtained for all of the species studied, including those for which analyses had been previously published.

The minerals in this family (Table 1) can be described as heteropolymolybdates, reflecting the fact that those structures that have been determined (the betpakdalite and obradovicite structure types) are made up of clusters of molybdate octahedra linked via other polyhedra ($Fe^{3+}O_6$ octahedra and arsenate or phosphate tetrahedra). The compositions and associations of paramendozavilite and the potentially new paramendozavilite-related mineral identified during this study strongly suggest that they also contain heteropolymolybdate frameworks.

References to heteropolymolybdates and to polyoxometalates date back to the work of Berzelius (Pope, 1983: pp. 101–107; Gouzerh and Che, 2006). In chemistry, a polyoxometalate (POM) is a polyatomic ion that consists of three or more transition metal oxyanions that are linked to form a cluster. If the cluster contains two or more different types of oxyanions, it is termed a heteropolyoxometalate. The best (and earliest) known heteropolymolybdate compound is ammonium phosphomolybdate, $(NH_4)_3[PMo_{12}O_{40}]$, which was described by Berzelius in 1826. The heteropolymolybdate cluster in this compound is the well known α-Keggin anion. It is important to note that our use of the term 'heteropolymolybdate' in reference to this family of minerals is different from the way it is normally used in chemistry. The structures of the minerals that are described here as heteropolymolybdates are based on infinite heteropolymolybdate frameworks, rather than isolated clusters.

In the first part of this report, we describe the investigations that led to the elucidation of the structural and crystal-chemical relationships between the members of the heteropolymolybdate family, we lay the groundwork for the description of new members of this family and present a suffix-based scheme for naming species. In the second part, we describe each of the existing

TABLE 1. Heteropolymolybdate minerals.

Original name	New name	Ideal formula
Betpakdalite	Betpakdalite-CaCa	$[Ca_2(H_2O)_{17}Ca(H_2O)_6][Mo_8As_2Fe^{3+}_3O_{36}(OH)]$
Natrobetpakdalite	Betpakdalite-NaCa	$[Na_2(H_2O)_{17}Ca(H_2O)_6][Mo_8As_2Fe^{3+}_3O_{34}(OH)_3]$
New	Betpakdalite-CaMg	$[Ca_2(H_2O)_{17}Mg(H_2O)_6][Mo_8As_2Fe^{3+}_3O_{36}(OH)]$
New	Betpakdalite-NaNa	$[Na_2(H_2O)_{16}Na(H_2O)_6][Mo_8As_2Fe^{3+}_3O_{33}(OH)_4]$
Mendozavilite	Mendozavilite-NaFe	$[Na_2(H_2O)_{15}Fe^{3+}(H_2O)_6][Mo_8P_2Fe^{3+}_3O_{35}(OH)_2]$
Melkovite	Melkovite	$[Ca_2(H_2O)_{15}Ca(H_2O)_6][Mo_8P_2Fe^{3+}_3O_{36}(OH)]$
New	Mendozavilite-NaCu	$[Na_2(H_2O)_{15}Cu^{2+}(H_2O)_6][Mo_8P_2Fe^{3+}_3O_{34}(OH)_3]$
New	Mendozavilite-KCa	$[K_2(H_2O)_{15}Ca(H_2O)_6][Mo_8P_2Fe^{3+}_3O_{34}(OH)_3]$
Obradovicite	Obradovicite-KCu	$[K_2(H_2O)_{17}Cu^{2+}(H_2O)_6][Mo_8As_2Fe^{3+}_3O_{34}(OH)_3]$
New	Obradovicite-NaCu	$[Na_2(H_2O)_{17}Cu^{2+}(H_2O)_6][Mo_8As_2Fe^{3+}_3O_{34}(OH)_3]$
New	Obradovicite-NaNa	$[Na_2(H_2O)_{16}Na(H_2O)_6][Mo_8As_2Fe^{3+}_3O_{33}(OH)_4]$
Paramendozavilite	Paramendozavilite	$[KAl_4(H_2O)_{30}][Mo_{12}P_6Fe^{3+}_6O_{60}(OH)_{13}]$

heteropolymolybdates briefly and fully describe six new members of the family. The foregoing text is based on a report on the heteropolymolybdate family, including the group and the suffix-based nomenclatures, which has been approved by the Commission on New Minerals, Nomenclature and Classification (CNMNC) of the International Mineralogical Association (Nomenclature Proposal 10-E). The six new minerals, betpakdalite-CaMg (IMA2011-034), betpakdalite-NaNa (IMA2011-078), mendozavilite-NaCu (IMA2011-039), mendozavilite-KCa (IMA2011-088), obradovicite-NaNa (IMA-2011-046), and obradovicite-NaCu (IMA-2011-079), described in the subsequent section have also been approved by the CNMNC.

PART I. OVERVIEW OF THE HETEROPOLYMOLYBDATE FAMILY

Elucidation of the heteropolymolybdate family

Powder X-ray diffraction studies

Powder X-ray diffraction patterns (Fig. 1) were recorded on a Rigaku R-Axis Rapid II large area curved imaging plate microdiffractometer with monochromatic Mo$K\alpha$ radiation using a Gandolfi-like motion on the φ and ω axes to randomize the sample orientation. The patterns for betpakdalite, natrobetpakdalite, mendozavilite, melkovite and four of the new phases were similar in all their major features, indicating they are isostructural. This fact has been confirmed by structure analyses for several of these phases (see below).

The pattern obtained from crystals from the obradovicite type specimen exhibits some similar features, suggesting that it has a related structure. Single-crystal structure determination on a crystal from the same specimen and one for a new Na-analogue of obradovicite (see below) confirmed the obradovicite structure to be related to that of betpakdalite, but to involve a different arrangement of structural components.

Paramendozavilite proved rather problematic. No material could be found on the type specimen (BM 1984,476) that yielded a powder pattern consistent with published powder data for paramendozavilite (Williams, 1986). Material on two other specimens of paramendozavilite (BM 1983,118 and NHMLAC 60464), which are henceforth considered to be neotypes (with approval of the CNMNC), provided patterns that are consistent with published powder data for paramendozavilite, although EMP analyses showed them to be K rather than Na dominant. The paramendozavilite pattern is different from those of betpakdalite and obradovicite. Crystals of paramendozavilite are twinned and too small for structure determination; however, a twinned crystal from NHMLAC 60464 yielded unit-cell parameters (see below). The crystals apparently mistaken for paramendozavilite on the original type specimen (BM 1984,476) are likely to be an undescribed molybdophosphate. The similar chemistry and close association of these phases

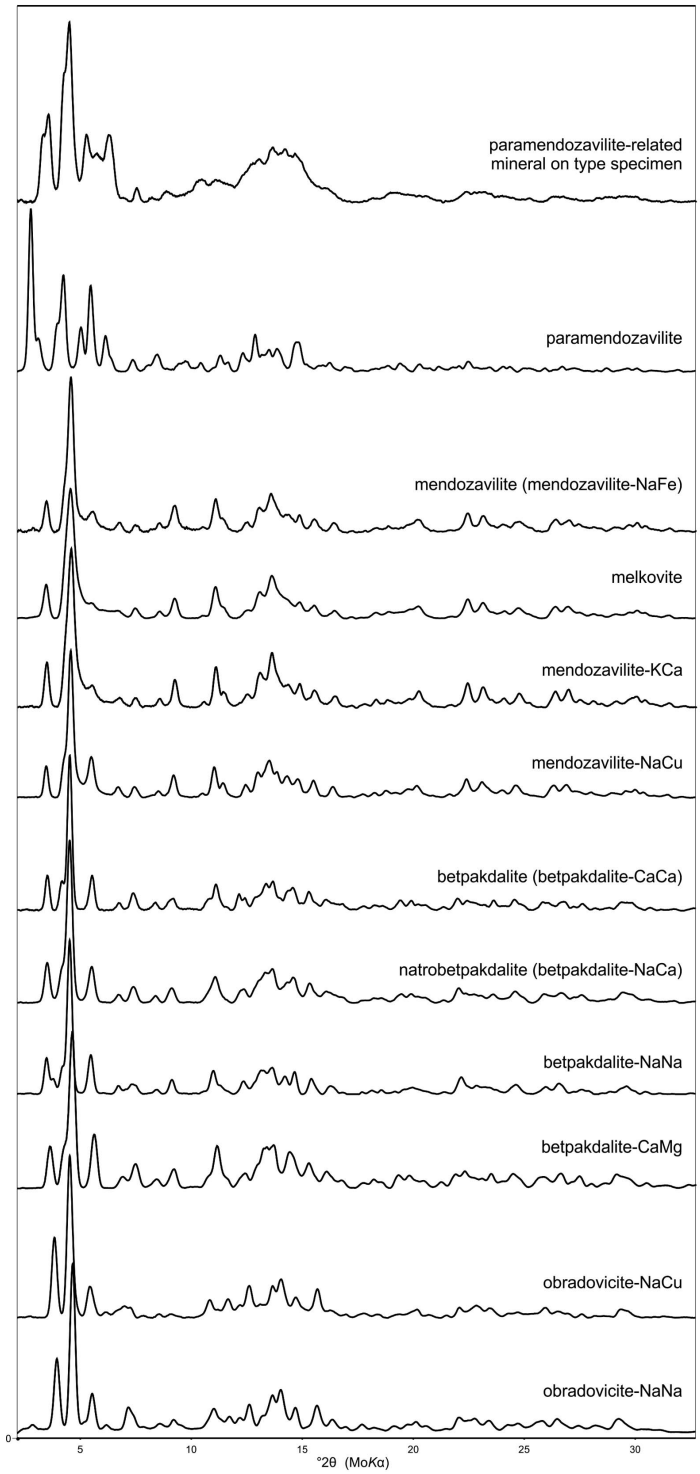

FIG. 1. Powder X-ray diffraction patterns for heteropolymolybdates.

with mendozavilite makes it highly likely that they contain similar molybdophosphate structural units. Similarities between the cell dimensions of mendozavilite and paramendozavilite are further evidence of a structural relationship.

Detailed listings of powder XRD data for the six new heteropolymolybdate species described herein have been deposited with the Editor of *Mineralogical Magazine* and can be downloaded from http://www.minersoc.org/pages/e_journals/dep_mat_mm.html.

Single-crystal studies and structure descriptions

Most of the single-crystal studies in the present investigation were done on a Rigaku R-Axis Rapid II large area curved imaging plate microdiffractometer with monochromatic Mo$K\alpha$ radiation. The sole exception was the data for the first structure determination, that of the new Na- and Cu-dominant molybdophosphate from Lomas Bayas mine, which was done at the ChemMatCARS, Sector 15, Advanced Photon Source at the Argonne National Laboratory, USA on a Bruker diffractometer using an APEX II CCD detector and radiation with a wavelength of 0.41328 Å.

Betpakdalite was first described from the Kara-Oba tungsten deposit in the Betpakdala desert, Kazakhstan by Ermilova and Senderova (1961). They reported an ideal formula of $CaFe_2H_4(As_2Mo_5O_{26})\cdot 12H_2O$, but noted that the correct formula could only be derived from determination of the structure. The structure of a mineral identified as betpakdalite was determined by Schmetzer *et al.* (1984) using material from Tsumeb, Namibia. Moore (1992) provided a detailed analysis of the betpakdalite structure based on this earlier determination, showing it to consist of a close-packed array of O atoms and voids. Cooper and Hawthorne (1999) reported a new structure determination using a better crystal, also from Tsumeb, provided by one of the authors (WWP). In the present study, we used better crystals (from the collection of WWP) of the material studied by Cooper and Hawthorne (1999) and obtained a new refinement that provided even better results (see below).

The structure of this betpakdalite consists of distinctive four-membered clusters of edge-sharing MoO_6 octahedra linked into a framework by sharing corners with other clusters, with $Fe^{3+}O_6$ octahedra and with AsO_4 tetrahedra. The framework corresponds to the close-packed array of O atoms described by Moore (1992). Open space within the framework is occupied by an $Mg(H_2O)_6$ octahedron (centred at [½;0;0]) and disordered Ca atoms and H_2O molecules. The structure is shown in Fig. 2. The chemistry of this 'betpakdalite' differs from that of type betpakdalite, which contains very little Mg (see below), and also differs from the material studied by Schmetzer *et al.* (1984), which contains significant K, Na and Zn.

A crystal from one of the cotype specimens of betpakdalite (FMM 62533) provided structure data from which the structure could be refined. Although twinning and inferior crystal quality did not provide as good a refinement, it did confirm that it possessed an identical framework and the same types of non-framework sites.

The structure determination of a Na-dominant molybdoarsenate from Chuquicamata, Antofagasta, Chile showed it to possess the same structural framework as betpakdalite. Its cell dimensions are nearly the same as those of betpakdalite, reflecting the fact that their frameworks are made up of the same atoms. Of the non-framework constituents, one Na occupies the site at [½;0;0] surrounded by six H_2O molecules in an octahedral configuration. The remaining Na atoms and H_2O molecules are disordered over numerous partially occupied sites in the channels.

The structure determination of the Na- and Cu-dominant molybdophosphate from the Lomas Bayas mine, Antofagasta, Chile, showed it to possess the same structural framework as betpakdalite, with P replacing As, and a small reduction in the size of the unit cell. Of the non-framework constituents, Cu^{2+} occupies the site at [½;0;0] and is surrounded by six H_2O molecules in an octahedral configuration. The partial occupancy of the site by Cu^{2+} and holosymmetric, rather than Jahn–Teller distorted, coordination are attributed to orientational averaging (see below). The Na atoms and remaining H_2O molecules are disordered over numerous partially occupied sites in the channels. The framework atoms refine very well at full occupancy; however, all non-framework atom positions indicated are fractionally occupied and significant additional electron density is distributed throughout the open space, indicating further disorder. A low quality refinement was also obtained for a new K- and Ca-dominated molybdophosphate with the betpakdalite structure.

A structure determination on a crystal of obradovicite from the type (possibly holotype)

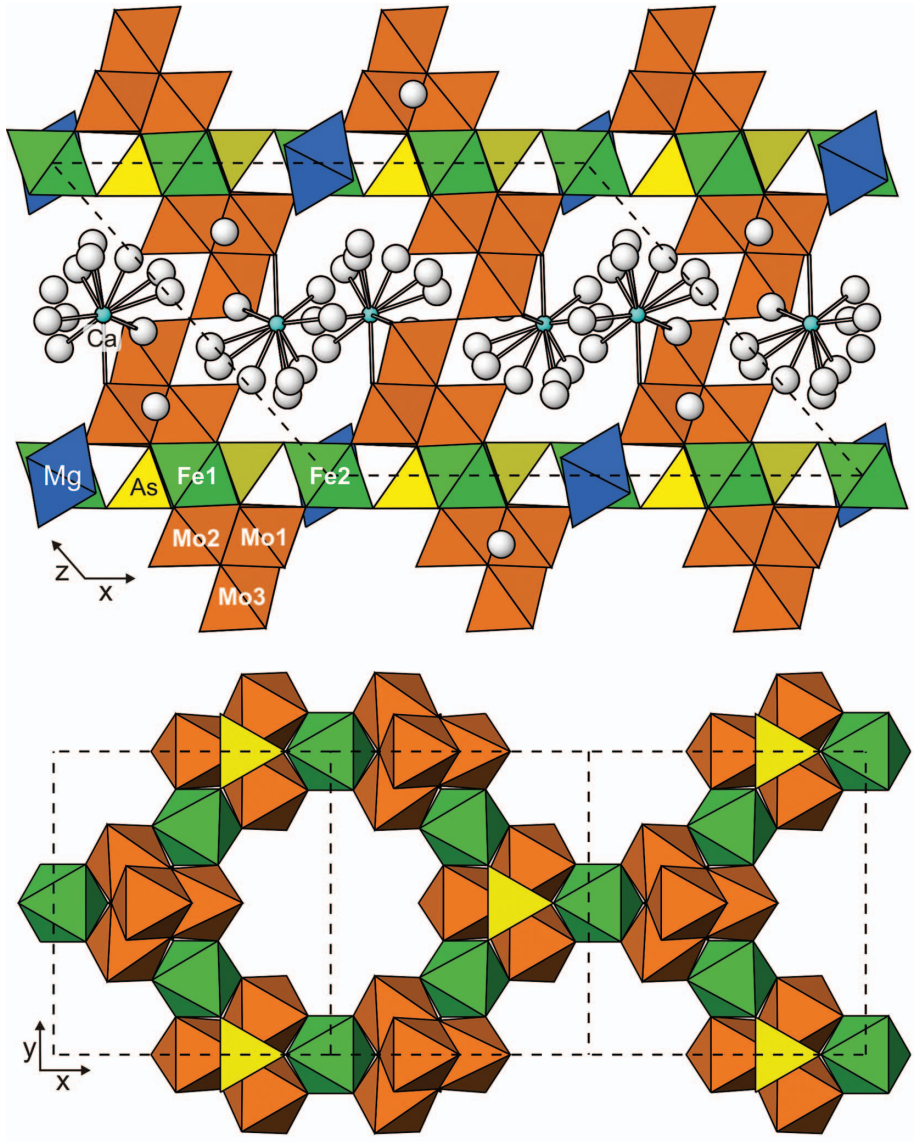

FIG. 2. Crystal structure of betpakdalite-CaMg. The upper projection is down [010] and shows the channel sites; the lower projection is on (001) and shows a single $[Mo_8As_2Fe^{3+}_3O_{36}(OH)]$ layer. Note the pseudo-trigonal symmetry of the $[Mo_8As_2Fe^{3+}_3O_{36}(OH)]$ layer, which probably accounts for the observed twinning.

specimen (CSM 86-496) showed it to possess a framework composed of the same distinctive four-member clusters of edge-sharing MoO_6 octahedra, linked together by sharing corners with other clusters, with $Fe^{3+}O_6$ octahedra and with AsO_4 tetrahedra; however, the linkage via one of the two $Fe^{3+}O_6$ octahedra (Fe1) is different from that of betpakdalite, leading to a framework with orthorhombic rather than monoclinic symmetry (Fig. 3). The obradovicite framework can be created from that of betpakdalite by reflection on $\{10\bar{1}\}$ or by 180º rotation about $[10\bar{3}]$ through the Fe1 octahedron (Fig. 4). This obradovicite structure contains a similar non-framework cation site at [0;0;½], partially occupied by Cu octahedrally coordinated to H_2O

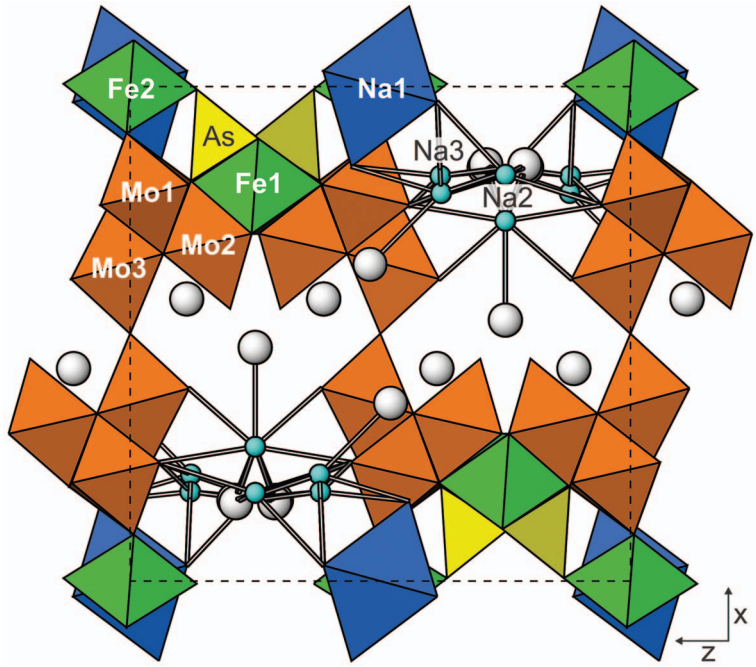

FIG. 3. Crystal structure of obradovicite-NaNa viewed down [010].

molecules, and it also contains sites partially occupied by Na/K and H_2O. The small size of the crystal used did not permit a high-quality refinement of the obradovicite structure; however, a new obradovicite species from Chuquicamata with Na as both of the dominant non-framework cations, provided an excellent refinement of the structure and showed Na to

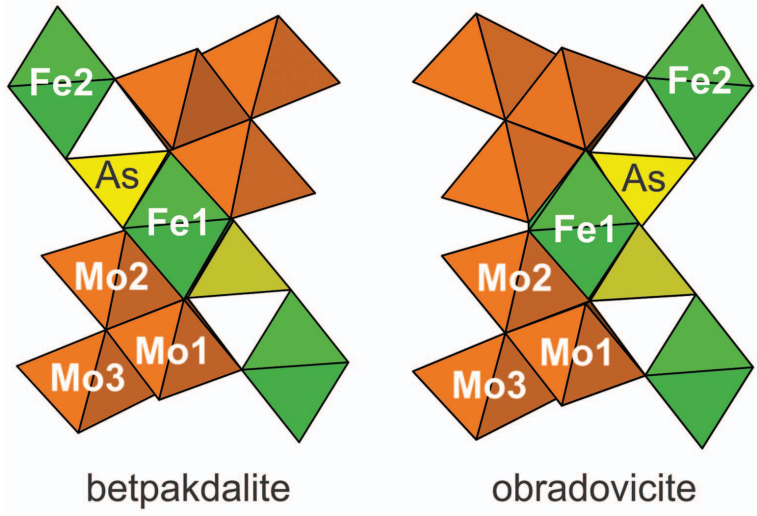

FIG. 4. Comparison of polyhedral linkages through the Fe1 octahedron in the betpakdalite and obradovicite structures. The obradovicite framework can be created from that of betpakdalite by reflection on $\{10\bar{1}\}$ (horizontal) or by 180° rotation about $[10\bar{3}]$ (approximately vertical) through the Fe1 octahedron.

occupy the non-framework site at [0;0;½] and Na and K atoms and additional H_2O molecules to be disordered over at least eight channel sites. In spite of the different framework linkage through the $Fe^{3+}O_6$ octahedra in the betpakdalite and obradovicite structure types and the different crystals systems (monoclinic *vs*. orthorhombic), the cell volumes are comparable and the cell contents (and ideal formulas) are the same. The details of the best refinements for each structure type, those for betpakdalite-CaMg, and obradovicite-NaNa, are reported in connection with the descriptions of those species (see below).

Note that bond-valence analyses (Table 8) for both structure types indicate that, without considering non-framework constituents, several framework O atoms have significantly low bond-valence sums. Considering the variable contents of channel cations, charge balance in these minerals can be achieved if OH replaces one or more framework O atoms.

Cell parameters

The cell parameters for all members of the heteropolymolybdate family are provided in Table 2. The cell parameters are based on single-crystal X-ray diffraction data (SCXRD) if possible; otherwise, the parameters have been refined from powder data either using *JADE 9.3* with whole-pattern fitting (PXRD-WPF; Materials Data, Inc.) or using *UnitCell* (PXRD; Holland and Redfern, 1995). It is worth noting that cell parameters are quite similar for species within each of the three groups (betpakdalite, mendozavilite and obradovicite; see below) reflecting the fact that the unit cells are dictated by the frameworks, and are affected very little by the non-framework constituents. Note that the cell volumes (Table 2) for the phosphates (mendozavilite group) range from 2379 to 2421 Å^3, whereas those for the arsenates (betpakdalite and obradovicite groups) range from 2464 to 2502 Å^3.

Group nomenclature

The nomenclature follows the recently approved definitions of Mills *et al.* (2009). A hierarchy can be established based on the following subdivisions: group, supergroup and family. Minerals with the betpakdalite structure can be divided into two groups: the betpakdalite group (As dominant) and the mendozavilite group (P dominant). These two groups make up the betpakdalite supergroup, named in accordance with the historical precedence (1961) of betpakdalite over mendozavilite (1982). Obradovicite and the new K- and Na-dominant molybdoarsenate with the obradovicite structure make up the obradovicite group. All of the minerals that contain (or are presumed to contain) a heteropolymolybdate framework are classified in the heteropolymolybdate family (Table 2).

Chemical compositions of betpakdalite and obradovicite supergroup minerals

Ideal formulae

Minerals of the betpakdalite, mendozavilite and obradovicite groups have the following general formula:

$[A_2(H_2O)_n B(H_2O)_6][Mo_8 T_2 Fe_3^{3+} O_{30+x}(OH)_{7-x}]$;

where:

(1) *A* is the dominant cation in the disordered channel sites. For simplicity, the total number of *A* cations is taken to be 2 in the ideal formula; however, the content varies from about 1 to 3.8 in analysed samples.

(2) *B* is the dominant cation at the octahedrally coordinated non-framework cation site. Ideally this site is fully occupied. The smallest of the non-framework cations generally occupies the *B* site; these cations can be monovalent, divalent or trivalent.

(3) *T* is the dominant cation (As or P) at the tetrahedrally coordinated framework site.

(4) *x* is equal to the total charge of the cations at the *A* and *B* sites, which ranges from 3 to 7 in the ideal formulae. Therefore, the number of framework O atoms that can be OH ranges from 0 to 4; however, because the content of the *A* site is highly variable and there can be deficiencies in the framework cations, empirical formulae can have OH >4.

(5) *n* is ideally 17 for arsenates and 15 for phosphates, if a medium-sized cation occupies the *B* site. This is based on structural evidence, which suggests that, discounting the non-framework octahedral coordination $[B(H_2O)_6]$, the remaining space in the non-framework portion (channels) of the structure is approximately two-thirds occupied by large cations and H_2O molecules. The frameworks of the arsenates (betpakdalite and obradovicite groups) have larger channel volumes than the phosphates (mendozavilite group) and consequently can have higher water contents. If a large cation, such as Na, occupies the *B* site, there is a decrease in the remaining void space in the

TABLE 2. Cell parameters for minerals of the heteropolymolybdate family.

	Original name	New name	Locality	Method	SG	*a* (Å)	b (Å)	c (Å)	β (º)	*V* (Å^3)
1	Betpakdalite	betpakdalite-CaCa	Betpakdala	SCXRD	*C*2/*m*	19.507(2)	11.0768(9)	15.2618(19)	131.488(5)	2470.3(5)
2	Betpakdalite	betpakdalite-CaCa	Descubridora	PXRD-WPF	*C*2/*m*	19.50(4)	11.15(5)	15.32(4)	131.30(9)	2502(14)
3	New	betpakdalite-CaMg	Tsumeb	SCXRD	*C*2/*m*	19.5336(7)	11.0637(4)	15.2559(11)	131.528(9)	2468.3(2)
4	Natrobetpakdalite	betpakdalite-NaCa	Kyzylsai	PXRD-WPF	*C*2/*m*	19.41(3)	11.12(4)	15.26(3)	131.13(7)	2481(11)
5	New	betpakdalite-NaNa	Chuquicamata	SCXRD	*C*2/*m*	19.2370(12)	11.0945(7)	15.1459(9)	130.342(1)	2463.8(3)
6	Mendozavilite	mendozavilite-NaFe	Cumobabi	PXRD-WPF	*C*2/*m*	18.82(12)	11.03(14)	15.18(12)	129.8(3)	2421(39)
7	Mendozavilite	mendozavilite-NaFe	Cumobabi	PXRD-WPF	*C*2/*m*	18.85(9)	10.99(11)	15.02(9)	129.9(2)	2387(30)
8	Mendozavilite	mendozavilite-NaFe	Lomas Bayas	PXRD-WPF	*C*2/*m*	18.86(12)	11.01(13)	15.07(12)	129.5(2)	2415(38)
9	Melkovite	melkovite	Shunak Mts.	PXRD-WPF	*C*2/*m*	18.81(9)	10.99(10)	15.11(9)	129.6(2)	2407(29)
10	New	mendozavilite-NaCu	Lomas Bayas	SCXRD	*C*2/*m*	18.9984(16)	10.9296(7)	15.0818(12)	129.906(2)	2402.3(3)
11	New	mendozavilite-KCa	Chuquicamata	SCXRD	*C*2/*m*	18.909(5)	10.897(2)	14.958(4)	129.780(9)	2368.6(10)
12	Obradovicite	obradovicite-KCu	Chuquicamata	PXRD*	*Pnmb*	14.848	11.056	15.046		2469.9
13	New	obradovicite-NaCu	Chuquicamata	SCXRD	*Pnmb*	14.872(4)	11.091(3)	15.032(4)		2479.4(12)
14	New	obradovicite-NaNa	Chuquicamata	SCXRD	*Pnmb*	14.8866(11)	11.0880(2)	15.0560(3)		2485.2(2)
15	Paramendozavilite	paramendozavilite	Cumobabi	PXRD	*monoclinic*	10.963(2)	25.881(3)	15.434(2)	110.73(1)	4095.8(6)
16	New	To be determined	Cumobabi	PXRD	*monoclinic*	10.936(6)	26.28(3)	13.17(2)	114.74(8)	3436(5)

The specimens used in these determinations are listed in the following table:

1	FMM 62533 (cotype)	5	NHMLAC #63570	9	NMNH 160237 (cotype)	13	CSM 86-496 (type)
2	NHMLAC 63312	6	NHMLAC 55475	10	NHMLAC 60483	14	NHMLAC 63313
3	NHMLAC 63327	7	BM 1984,475 (cotype)	11	NHMLAC 63315	15	NHMLAC 60464
4	FMM 47275 (cotype)	8	NHMLAC 60483	12	Finney et al. (1986)	16	BM 1984,476

* Cell parameters from Finney *et al.* (1986) transformed to correspond to our cell.

channels and, consequently, the maximum water content is reduced by ~1 water molecule per formula unit. In these cases, *n* is ideally 16 for arsenates and 14 for phosphates.

The high degree of variability in channel cation and H_2O content means that empirical formulae sometimes deviate considerably from generalized ideal formulae. For example, an excess or deficiency in the ideal number of *A* cations will theoretically decrease or increase (respectively) the maximum water content.

Calculation of crystal-chemical formulae

Obtaining an accurate and meaningful analysis of betpakdalite-, mendozavilite- and obradovicite-group minerals is not a trivial task. These minerals are commonly unstable under an electron beam and may also undergo partial dehydration in vacuum. Nevertheless, good analyses can be obtained in appropriate conditions. During these studies, electron microprobe analyses were performed under the following conditions: an accelerating voltage of 15 kV and a beam current of 5 nA with a defocussed beam (the beam diameter had to be reduced in some cases because of the small sample size). Counting times of 20 s for the peaks and 10 s for the background were used. The lines and standards used were: Na*K*α, albite; Al*K*α, kyanite; Si*K*α, kyanite; P*K*α, fluorapatite; K*K*α, K-feldspar; Ca*K*α, diopside; Mg*K*α, diopside; Fe*K*α, fayalite; Cu*K*α, tennantite; As*L*α, tennantite; and Mo*L*α, Mo metal.

In most cases it was not possible to make a direct determination of the H_2O content due to the small amount of material and/or the difficulty in separating a pure sample; therefore, an exact chemical formula must take into account crystal-chemical considerations in determining the maximum H_2O content (as described above) in the absence of a crystal-structure determination. As a result of the generally high degree of disorder in the non-framework part of the structure, information about the water content derived from crystal-structure determinations is usually incomplete.

Given a set of chemical analyses of a mineral in the betpakdalite, mendozavilite or obradovicite group, the following criteria may be used to derive an empirical formula:

(1) Calculation on the basis of Mo = 8. Extensive examination shows that Mo occurs at the only site in which little, if any, substitution occurs. As Mo is bound strongly in the framework the Mo content tends to be constant. In cases in which the assumption Mo = 8 produces P + As (+ Si) > 2, it is preferable to calculate the formula based on P + As (+ Si) = 2 (and have a slight resultant deficiency in Mo).

(2) The content at the framework Fe site is assigned such that Fe^{3+} + Al = 3; the Fe^{3+} is assigned to this site first, followed by Al. Any excess Fe or Al must then be distributed over the channel sites. Unless there is definite evidence to the contrary, all Fe is assumed to be Fe^{3+}.

(3) Full occupancy (one) is assumed for the non-framework *B* site. The smallest cations are placed in this site.

(4) Excess small cations that cannot be accommodated at the *B* site, plus all remaining cations (generally monovalent and divalent) are placed at the non-framework *A* sites. The total occupancy of these disordered sites can range between 1 and 3.8 cations p.f.u.

(5) For reliable determination of the total H_2O content, direct determination by CHN (or similar techniques) is generally necessary. If a reliable direct determination of H_2O is not possible, but the density can be measured accurately, the H_2O content should be based on the measured density. As noted above, evidence for H_2O content from crystal structure determination is usually inconclusive because the channel constituents always exhibit substantial disorder and partial occupancy, and the identification of cation *vs.* water at specific sites can be ambiguous. The determination of water by difference from EMP analyses is not reliable because of the instability of these minerals in the electron beam. If water has been directly determined, it is generally best to normalize the EMP analyses, so that they total 100% with the determined water content. In the absence of an accurate direct water determination or a reliable density measurement, water should be calculated based on the estimated limits of channel occupancy, as described above. If the water content is calculated in this way, allowance should be made for the number of cations assigned to the *A* sites, as a cation excess (>2) at these sites will result in a corresponding reduction in the maximum water content, and a cation deficiency (<2) at these sites will result in a corresponding increase in the maximum water content. Some of the 37 framework O atoms may need to be assigned as OH to maintain charge balance.

Unless otherwise noted, the H_2O contents in the empirical formulas provided for the heteropoly-

molybdate species listed in Part II (below) are based on the estimated limits of channel occupancy.

Discrimination of species

Powder X-ray diffraction serves well for discriminating between heteropolymolybdates with different structures and it is generally sufficient for distinguishing between phosphates and arsenates with the same structure. Chemical information is required to distinguish between species within groups. Infrared and Raman spectroscopy is not likely to be useful in this respect because the distinctions are based on non-framework cation constituents and there is the further complication of significant disorder.

Although detailed electron-microprobe analyses are recommended for accurate determinations, energy-dispersive spectrometry or other semi-quantitative chemical analytical methods may suffice. Particular caution must be exercised in studying those species that may have Fe as a non-framework cation as Fe is invariably a major constituent of the framework.

Suffix-based nomenclature

In the suffix-based nomenclature scheme for minerals of the betpakdalite, mendozavilite and obradovicite groups, the group name is the root name, and the two dominant non-framework cations (*A* and *B*) are provided in a suffix of the form: *-AB*. If phosphates with the obradovicite structure are discovered, a new root name will be required. If no structure determination has been made, it is assumed that the smaller of the two non-framework cations is at the *B* site. The use of this suffix-based nomenclature eliminates the need to introduce trivial names for six new species that have been identified in the course of this study. We have chosen mendozavilite rather than melkovite as the root name for phosphates with the betpakdalite structure despite that fact that melkovite has priority (1969 *vs.* 1986) as (1) mendozavilite has previously been reported from more localities than melkovite (three *vs.* one) and there are many more references to it in the literature; and (2) the use of melkovite as the root name would leave paramendozavilite as something of an orphan and it seemed inappropriate to rename it paramelkovite. Although the suffix-based nomenclature logically requires the renaming of melkovite as mendozavilite-CaCa, the name melkovite has been retained as the official name for the species for historical reasons, in keeping with current CNMNC guidelines (Hatert *et al*., in press).

The Gladstone–Dale compatibilities of the heteropolymolybdates

In most cases, the heteropolymolybdates have poor to only marginally good Gladstone–Dale compatibility indices (Mandarino, 1981). The compatibilities for 9 out of 11 heteropolymolybdates fall in the range −0.059 to −0.124 (Table 4*b*). We believe that this is due to an incorrect Gladstone–Dale constant ($k = 0.237$) for Mo^{6+} in the edge-sharing octahedral clusters. Using our relatively small statistical sampling, we suggest an improved constant for MoO_3 in heteropolymolybdates of 0.280. If this is used in the calculations, all nine of the heteropolymolybdates with original Gladstone–Dale compatibilities in the poor to marginally good range, have compatibilities in the excellent to superior range (Table 4*b*). The compatibilities for mendozavilite-NaFe and paramendozavilite are significantly worse using the new value, and we believe that the data for these minerals (Williams, 1986) deserve further scrutiny.

PART II. MINERALS OF THE HETEROPOLYMOLYBDATE FAMILY

Betpakdalite supergroup: betpakdalite group

Betpakdalite – new suffix-based name: betpakdalite-CaCa

$[Ca_2(H_2O)_{17}Ca(H_2O)_6][Mo_8As_2Fe^{3+}_3O_{36}(OH)]$

Betpakdalite was first described from the Kara-Oba tungsten deposit in the Betpakdala desert, Kazakhstan (47º16′N, 72º15′E) by Ermilova and Senderova (1961). They reported an ideal formula $CaFe_2H_4(As_2Mo_5O_{26})\cdot 12H_2O$, but noted that the correct formula could only be derived from determination of the structure. Better crystals from Tsumeb, Namibia, allowed Schmetzer *et al.* (1984) to determination the crystal structure. Moore (1992) provided a detailed analysis of the betpakdalite structure based on this earlier determination, showing it to consist of a close-packed array of O atoms and voids and pointing out the unlikely assignment of K to the octahedrally-coordinated non-framework site (*B* site). The chemical analyses provided by Schmetzer *et al.* (1984) have a range of

compositions from betpakdalite-CaCa to *betpakdalite-KCa*, the latter being a probable new group member on theoretical grounds that was not found during this study and, consequently, has not been described as a new species. Cooper and Hawthorne (1999) redetermined the betpakdalite structure using better crystals from Tsumeb; this material has a chemistry corresponding to betpakdalite-CaMg (see below).

In the course of the present study, we obtained EMPA, PXRD and single-crystal XRD data for cotype material from the Fersman Mineralogical Museum (FMM 62533). The EMPA data (Table 3*a*) showed some significant differences (much lower As_2O_5 and much higher MoO_3) from those reported by Ermilova and Senderova (1961); however, both analyses are consistent with betpakdalite-CaCa. Our EMPA provided the empirical formula $[(Ca_{0.74}Na_{0.17}K_{0.11})_{\Sigma 1.02}(H_2O)_{17.98}(Ca_{0.99}Cu^{2+}_{0.01})_{\Sigma 1.00}(H_2O)_6][Mo_8(As_{1.74}P_{0.04}Si_{0.02})_{\Sigma 1.80}(Fe^{3+}_{2.89}Al_{0.01})_{\Sigma 2.90}O_{32.44}(OH)_{4.56}]$. The PXRD pattern (Fig. 1) is consistent with those obtained from other betpakdalite-group minerals. We were able to refine the structure based on single-crystal XRD data [$R_1 = 0.0985$ for 1557 $F_o > 4\sigma F$]. Although the quality of these data did not permit accurate determination of the non-framework sites, the essential details of the structure are consistent with the other refinements of the betpakdalite structure and with type betpakdalite corresponding to betpakdalite-CaCa.

In the course of this study, we also examined material corresponding to betpakdalite-CaCa from four other localities: the Descubridora mine, Pampa Larga district, Copiapó, Chile (NHMLAC 63312); Bajan Cogto, Mongolia (NHMLAC 63997); the Rustler mine, Gold Hill district, Tooele County, Utah, USA (NHMLAC 63998); and the Nedre Kvartsen quarry, Drag, Tysfjord, Nordland, Norway (NHMLAC 63999). The EMPA for the material from the Descubridora mine (Table 3*a*) yields the empirical formula $[(Ca_{0.86}Na_{0.36}K_{0.21})_{\Sigma 1.43}(H_2O)_{17.57}(Ca_{0.99}Cu^{2+}_{0.01})_{\Sigma 1.00}(H_2O)_6][Mo_8As_{1.88}(Fe^{3+}_{2.76}Al_{0.05})_{\Sigma 2.81}O_{33.12}(OH)_{3.88}]$.

Natrobetpakdalite – new suffix-based name: betpakdalite-NaCa

$[Na_2(H_2O)_{17}Ca(H_2O)_6][Mo_8As_2Fe^{3+}_3O_{34}(OH)_3]$

Skvortsova *et al.* (1971) described sodium betpakdalite from the Kyzylsai Mo-U deposit, Chu-Ili mountains, Kazakhstan. The name change to natrobetpakdalite was announced by Burke (2008). We obtained cotype material from the Fersman Mineralogical Museum (FMM 47275). Although crystals from this cotype specimen were not of sufficient size or quality for single-crystal XRD study, the PXRD pattern (Fig. 1) is clearly consistent with those obtained from other betpakdalite-group minerals. The EMPA data (Table 3*a*) showed some significant differences (lower Na_2O and As_2O_5 and higher MoO_3) compared to the data reported by Skvortsova *et al.* (1971); however, both analyses are consistent with this material corresponding to betpakdalite-NaCa. The empirical formula based on our EMPA is $[(Na_{1.10}Ca_{0.47}K_{0.14})_{\Sigma 1.71}(H_2O)_{17.29}(Ca_{0.93}Al_{0.05}Cu^{2+}_{0.02})_{\Sigma 1.00}(H_2O)_6][Mo_8As_{1.88}(Fe^{3+}_{2.78}Al_{0.22})_{\Sigma 3.00}O_{33.63}(OH)_{3.37}]$.

Betpakdalite-CaMg (IMA2011-034) – new species

$[Ca_2(H_2O)_{17}Mg(H_2O)_6][Mo_8As_2Fe^{3+}_3O_{36}(OH)]$

Betpakdalite-CaMg occurs on the 35th level of the world famous Tsumeb mine, Tsumeb, Namibia (19º15′S, 17º42′E), which is the type locality for approximately 60 other minerals [an overview of the mineralogy of the Tsumeb deposit can be found in Gebhard (1999)]. Crystals of betpakdalite-CaMg from this occurrence provided by one of the authors (WWP) were first investigated by Cooper and Hawthorne (1999) in their structure determination of 'betpakdalite', although this material differs significantly in chemistry from that of type betpakdalite (see above; Ermilova and Senderova, 1961). The crystals occur as inclusions in large scorodite crystals.

In our study, we examined crystals from the same specimen that yielded the crystals used by Cooper and Hawthorne, and better crystals from another specimen in the collection of WWP. Vials containing these crystals, numbered 63328 and 63327, respectively, are designated as the cotypes and are deposited in the collections of the Natural History Museum of Los Angeles County. Based on the virtually identical appearances, compositions and associations of the material, it is very likely that the two specimens came from the same pocket. Betpakdalite-CaMg occurs on and included in scorodite, with associated quartz and djurleite. It is an oxidation zone mineral which is presumed to have formed as a result of the alteration of As, Fe and Mo sulfides by solutions rich in Ca and Mg.

TABLE 3*a*. Chemical analyses of betpakdalite group minerals.

Original name	Betpakdalite	Betpakdalite	Betpakdalite	Betpakdalite	Natro-betpakdalite	Natro-betpakdalite	New	New	New
New name	Betpakdalite-CaCa	Betpakdalite-CaCa	Betpakdalite-CaCa	Betpakdalite-CaCa to *KCa*	Betpakdalite-NaCa	Betpakdalite-NaCa	Betpakdalite-CaMg	Betpakdalite-CaMg	Betpakdalite-NaNa
Locality	Betpakdala	Betpakdala	Descubridora	Tsumeb	Kyzylsai	Kyzylsai	Tsumeb	Tsumeb	Chuquicamata
Analysis	Ermilova and Senderova, 1961 (wet chem.; DTA)	This study (EMPA measured/ normalized)	This study (EMPA measured/ normalized)	Schmetzer *et al.*, 1984 (EMPA)	Skvortsova *et al.*, 1971 (wet chem.; DTA)	This study (EMPA measured/normalized)	Cooper and Hawthorne, 1999 (EMPA)	This study (EMPA measured/ normalized)	This study (EMPA measured/ normalized; CHN)
Na_2O		0.28/0.25	0.58/0.52	0.20−0.48	3.14	1.60/1.58		0.64/0.60	5.94/5.45
K_2O		0.28/0.25	0.50/0.45	0.51−3.52	0.20	0.30/0.30		0.21/0.20	1.62/1.49
CaO	4.14	5.05/4.48	5.33/4.76	5.21−6.10	4.23	3.68/3.64	5.3	5.20/4.85	0.13/0.12
SrO									
ZnO				0.38−0.96					
CuO		0.06/0.05	0.04/0.04			0.06/0.06		0.12/0.11	0.21/0.19
MgO					0.22		1.8	2.00/1.86	
Fe_2O_3	11.70	12.00/10.65	11.32/10.12	11.3−12.6	11.25	10.40/10.28	11.2	11.79/10.99	12.15/11.15
Al_2O_3		0.02/0.02	0.12/0.11		0.40	0.65/0.64		0.02/0.02	0.01/0.01
SiO_2		0.07/0.06	0.04/0.04		0.20			0.12/0.11	
TiO_2									
ZrO_2									
P_2O_5		0.03/0.03	0.01/0.01					0.20/0.19	1.11/1.02
As_2O_5	14.86	10.40/9.23	11.12/9.94	9.0−10.1	13.93	9.48/9.38	10.0	10.15/9.46	8.54/7.84
MoO_3	50.24	59.89/53.15	59.19/52.91	52.3−55.2	50.22	53.89/53.29	52.9	56.48/52.62	58.75/53.94
WO_3				0.55−1.45					
Cl									
$O \equiv Cl$									
H_2O_{meas}	19.00	n.d.	n.d.	n.d.	16.65	n.d.	n.d.	n.d.	14.71
H_2O_{den}								21.72	20.19
H_2O_{the}		24.61/21.84*	23.62/21.11*			21.06/20.83*	19.2	20.40/19.01*	20.46/18.78*
Total	99.94	112.69/100.01	111.87/100.01		100.44	101.12/100.00	100.6	107.33/100.00	108.92/99.99

The H_2O content is provided in three separate ways: H_2O_{meas} is the analytically determined H_2O content; H_2O_{den} is the calculated H_2O content based on the measured density; H_2O_{the} is the theoretical maximum H_2O content based on packing considerations.
* The H_2O content used for the calculation of our empirical formulae.
n.d.: not determined.

TABLE 3*b*. Chemical analyses of mendozavilite group minerals.

Original name	Mendozavilite	Mendozavilite	Mendozavilite	Melkovite	Melkovite	Melkovite	New	New
New name	*Mendozavilite-CaFe*	Mendozavilite-NaFe	Mendozavilite-NaFe	Melkovite	Melkovite	Melkovite	Mendozavilite-NaCu	Mendozavilite-KCa
Locality	Cumobabi	Cumobabi	Lomas Bayas	Shunak Mts.	Shunak Mts.	Fitzgerald R.	Lomas Bayas	Chuquicamata
Analysis	Williams, 1986 (wet chemistry)	This study (EMPA measured/ normalized)	This study (EMPA measured/ normalized)	Yegorov et al., 1969 (wet chem.; DTA)	This study (EMPA measured/ normalized)	Birch *et al*., 2002 (EMPA)	This study (EMPA measured/ normalized; CHN)	This study (EMPA measured/ normalized; CHN)
Na_2O	1.25	1.99/1.78	1.15/1.04	1.12	0.83/0.77	1.07/0.95	2.75/2.44	1.90/1.75
K_2O		2.83/2.54	0.25/0.23	0.28	0.18/0.17	0.35/0.31	0.08/0.07	3.67/3.37
CaO	2.48	4.27/3.83	0.06/0.05	5.15	6.64/6.15	5.12/4.53	0.11/0.10	3.30/3.03
SrO						0.36/0.32		
ZnO								
CuO		0.13/0.12	0.03/0.03		0.06/0.06		4.71/4.18	0.22/0.20
MgO	0.35	0.14/0.13	1.11/1.01			0.42/0.37	0.59/0.52	
Fe_2O_3	14.31	14.20/12.73	19.04/17.28	10.90	11.19/10.37	12.92/11.44	12.45/11.06	13.09/12.04
Al_2O_3	0.76	0.40/0.36	0.02/0.02		0.01/0.01		0.02/0.02	0.04/0.04
SiO_2		0.17/0.15	0.01/0.01		0.20/0.19		0.02/0.02	0.03/0.03
TiO_2								
ZrO_2				0.97				
P_2O_5	6.78	7.27/6.52	6.81/6.18	7.86	6.44/5.97	7.70/6.82	7.31/6.49	7.21/6.63
As_2O_5					0.08/0.07			0.34/0.31
MoO_3	50.47	58.90/52.81	60.86/55.25	57.17	60.11/55.72	62.43/55.28	63.45/56.36	62.93/57.86
WO_3								
Cl	0.26	0.16/0.14						
$O \equiv Cl$		−0.04/−0.04						
H_2O_{meas}	21.62	n.d.	n.d.	16.59	n.d.	n.d.	15.19	12.15
H_2O_{den}							21.08/18.73*	16.03/14.74*
H_2O_{the}		21.12/18.93*	20.82/18.90*		22.14/20.52*	22.57/19.98*	22.94	21.22
Total	98.28	111.54/100.00	110.16/100.00	100.04	107.88/100.00	112.94/100.00	112.57/99.99	108.76/100.00

The H_2O content is provided in three separate ways: H_2O_{meas} is the analytically determined H_2O content; H_2O_{den} is the calculated H_2O content based on the measured density; H_2O_{the} is the theoretical maximum H_2O content based on packing considerations.
* The H_2O content used for the calculation of our empirical formulae.
n.d.: not determined.

TABLE 3*c*. Chemical analyses of obradovicite group and paramendozavite-related minerals.

Original name	Obradovicite	New	New	Para-mendozavilite	Para-mendozavilite	New
New name	Obradovicite-KCu	Obradovicite-NaCu	Obradovicite-NaNa	Para-mendozavilite	Para-mendozavilite	To be determined
Locality	Chuquicamata	Chuquicamata	Chuquicamata	Cumobabi	Cumobabi	Cumobabi
Analysis	Finney *et al*., 1986 (wet chemistry)	This study (EMPA measured/ normalized)	This study (EMPA measured/ normalized; CHN)	Williams, 1986 (wet chemistry)	This study (EMPA measured/ normalized)	This study (EMPA)
Na_2O	0.56	3.37/2.97	5.03/4.35	0.54	0.08/0.07	
K_2O	2.48	4.15/3.66	4.01/3.47		0.72/0.72	0.87
CaO		0.18/0.16	0.08/0.07	0.59	0.16/0.16	0.06
SrO						
ZnO			0.05/0.04			
CuO	5.85	2.35/2.07	0.45/0.39			
MgO				0.16	0.14/0.14	0.17
Fe_2O_3	10.12	13.20/11.64	12.63/10.93	13.36	13.41/13.35	13.22
Al_2O_3		0.01/0.01		4.65	5.73/5.70	5.59
SiO_2		0.02/0.02				0.01
TiO_2					0.29/0.29	0.01
ZrO_2						
P_2O_5		0.26/0.23	0.18/0.16	10.32	11.28/11.23	10.86
As_2O_5	8.46	10.39/9.16	11.07/9.58			
MoO_3	55.29	58.93/51.97	61.29/53.06	42.01	49.23/49.01	47.62
WO_3						
Cl				0.65	0.16/0.16	0.26
$O \equiv Cl$						
H_2O_{meas}	18.33	n.d.	15.07	28.05	n.d.	n.d.
H_2O_{den}						
H_2O_{the}		20.53/18.11*	20.73/17.95*		19.29/19.20*	
Total	101.09	113.39/100.00	115.52/100.00	100.33	100.45/100.00	

The H_2O content is provided in three separate ways: H_2O_{meas} is the analytically determined H_2O content; H_2O_{den} is the calculated H_2O content based on the measured density; H_2O_{the} is the theoretical maximum H_2O content based on packing considerations.
* The H_2O content used for the calculation of our empirical formulae.
n.d.: not determined.

The crystals of betpakdalite-CaMg are yellow pseudo-octahedra up to ~1 mm in maximum dimension (Fig. 5). They exhibit the forms {001}, $\{1\bar{1}0\}$ and $\{20\bar{1}\}$ (Fig. 6). In contrast to the other members of the betpakdalite supergroup in which twinning is very common, twinning is uncommon in betpakdalite-CaMg. It was noted as contact twins on (001) by rotation of 120º about [102] and as penetration twins, also by rotation of 120º about [102]. The physical and optical properties are listed in Tables 4*a* and 4*b*, respectively.

The EMPA reported by Cooper and Hawthorne (1999) is provided in Table 3a, as is our very similar EMPA on crystals from the second specimen. The analyses are consistent with the new species, betpakdalite-CaMg. The empirical formula based on our EMPA is $[(Ca_{1.89}Na_{0.42}K_{0.09}Cu^{2+}_{0.03}Mg_{0.01}Fe^{3+}_{0.01}Al_{0.01})_{\Sigma 2.46}(H_2O)_{16.53}Mg_{1.00}(H_2O)_6][Mo_8(As_{1.80}P_{0.06}Si_{0.04})_{\Sigma 1.90}Fe^{3+}_{3.00}O_{35.89}(OH)_{1.11}]$. The PXRD pattern (Fig.1) is consistent with those of other betpakdalite-group minerals.

We collected new structure data on a crystal from the second specimen described above and obtained an excellent refinement [R_1= 0.0213 for 3880 $F_o > 4\sigma F$]. This is by far the best structure

TABLE 4*a*. Physical properties of members of the heteropolymolybdate family.

Data source	Betpakdalite-CaCa Ermilova and Senderova, 1961	Betpakdalite-NaCa Skvortsova *et al*., 1971	Betpakdalite-CaMg This study	Betpakdalite-NaNa This study	Mendozavilite-NaFe Williams, 1986	Melkovite Yegorov *et al*., 1969	Mendozavilite-NaCu This study	Mendozavilite-KCa This study	Obradovicite-KCu Finney *et al*., 1986	Obradovicite-NaCu This study	Obradovicite-NaNa This study	Paramendozavilite Williams, 1986
Colour	lemon yellow with greenish tint	lemon yellow	yellow	yellow	Empire yellow to orange	brownish yellow; lemon yellow	lime green	greenish yellow	pea green	yellowish green	yellowish green	pale yellow
Streak	n.d.	n.d.	colourless to very pale yellow	colourless to very pale yellow	bright yellow	n.d.	colourless to very pale green	very pale greenish yellow	pale pea green	very pale yellowish green	very pale yellowish green	very pale yellow
Lustre	dull to waxy	dull	vitreous to sub-adamantine	vitreous to sub-adamantine	vitreous	dull to waxy	vitreous to sub-adamantine	vitreous to sub-adamantine	vitreous to sub-adamantine	vitreous to sub-adamantine	vitreous to sub-adamantine	vitreous
Transparency	transparent	semi-transparent	transparent	transparent	semi-transparent	transparent	transparent	transparent	translucent	transparent	transparent	semi-transparent
Fluorescence	n.d.	n.d.	none	none	none	none	none	none	none	none	none	
Hardness (Mohs)	~3	n.d.	~3½	~3	1½	~3	~2½	~2½	2½	~2	~2	1
Fracture		n.d.	irregular	splintery	n.d.		irregular	irregular	not reported	splintery	splintery	n.d.
Tenacity		n.d.	brittle	brittle	n.d.	brittle	slightly flexible; not elastic	brittle	not reported	brittle	brittle	n.d.
Cleavage	{001} very good	n.d.	{001} perfect	{001} perfect	n.d.	one perfect	{001} perfect	{001} perfect	none	none	none	one perfect
D_{meas} (g cm^{-3})	2.98–3.05	2.02	2.98(4)	2.87(3)	3.85	2.969–2.973	2.824(5)	2.79(2)	3.55(5)	n.d.	n.d.	3.35
D_{calc} (g cm^{-3})	2.913	2.892	2.944	2.877	2.948	2.851	2.824	2.790	2.830	2.967	2.900	2.858
Chemical tests	n.d.	n.d.	slowly decomp. in dil. HCl	slowly sol. in conc. HCl	easily sol. in dil. acids	easily sol. in dil. acids	slowly sol. in conc. HCl	slowly sol. in conc. HCl	readily sol. in 1:1 HCl	slowly sol. in dil. HCl	slowly sol. in dil. HCl	easily sol. in dil. acids

The densities of obradovicite-NaCu and obradovicite-NaNa could not be measured because the crystals react with aqueous density liquids. All calculated densities are based on the chemical analyses and unit-cell determinations obtained in this study, except for that of obradovicite-KCu, which is based on data from Finney *et al*. (1986). For mendozavilite-NaCu and mendozavilite-KCa, the H_2O contents were based on the measured density, so the measured and calculated densities are equivalent; n.d. is not determined.

TABLE 4*b*. Optical properties of members of the heteropolymolybdate family.

	Betpakdalite-CaCa	Betpakdalite-NaCa	Betpakdalite-CaMg	Betpakdalite-NaNa	Mendozavilite-NaFe	Melkovite	Mendozavilite-NaCu	Mendozavilite-KCa	Obradovicite-KCu	Obradovicite-NaCu	Obradovicite-NaNa	Paramedozavilite
Data source	Ermilova and Senderova, 1961	Skvortsova *et al*., 1971	This study	This study	Williams, 1986	Yegorov *et al*., 1969	This study	This study	Finney *et al*., 1986	This study	This study	Williams, 1986
Optics	biaxial (+)	biaxial	biaxial (+)	biaxial (+)	biaxial (+)	n.d.	biaxial (+)	biaxial (+)	biaxial (+)	biaxial (−)	biaxial (+)	biaxial (−)
α	1.782−1.809	1.792	1.818(3)	1.765(5)	1.762	n.d.	1.770(5)	1.780(5)	1.790	1.790(3)	1.768(3)	1.686
β	1.797−1.821	n.d.	1.824(3)	1.785(5)	1.763	1.838 (av)	1.785(5)	1.795(5)	1.798	1.798(3)	1.776(3)	1.710
γ	1.850−1.857	1.81	1.846(3)	1.850(calc)	1.766	n.d.	1.805(5)	1.817(calc)	1.811	1.805(calc)	1.787(3)	1.720
$2V_{meas}$ (°)	n.d.	n.d.	55(2)	60(5)	5−15 (2*E*)	n.d.	80(10)	80(10)	81	86(5)	82(2)	60 (2*E*)
$2V_{calc}$ (°)	53−88°		55.7	–	60.1	–	82.6	–	75.7	–	81.4	64.9
Dispersion	extreme, inclined	n.d.	$r < v$, strong	$r < v$, moderate	$r > v$, extreme	n.d.	$r < v$, strong, inclined	$r < v$, strong	$r > v$, extreme	$r > v$, strong	$r < v$, strong	n.d.
Orientation	Y = **b**; X ^ **c** = 12°	Z^elongation = 38°	Y = **b**, $Z \approx$ **c**, $X \approx$ **a***	Y = **b**, X ^ **a** = 60° in obtuse β	n.d.	n.d.	Y = **b**, $X \approx$ **c**, $Z \approx$ **a***	Y = **b**, $X \approx$ **c**, $Z \approx$ **a***	X = **a**, Y = **b**, Z = **c**	X = **a**, Y = **b**, Z = **c**	X = **a**, Y = **b**, Z = **c**	n.d.
Pleochroism	X pale yellow, Y greenish yellow, Z bluish; $Z > Y > X$	X pale yellow, Z yellow; $Z > X$	none	none	pale yellow; $Z > Y > X$	weak; colourless to light green	pale olive green; $Y > X = Z$	none	weak; yellow; $Z > X = Y$	none	none	pale yellow; $Z > Y > X$
Gladstone−Dale Compatibility k (MoO_3) = 0.237	−0.085 poor	−0.076 fair	−0.102 poor	−0.089 poor	0.003 superior	−0.127 poor	−0.083 poor	−0.122 poor	−0.121 poor	−0.061 fair	−0.059 good	0.051 good
Gladstone−Dale Compatibility k (MoO_3) = 0.280	0.003 superior	0.012 superior	−0.013 superior	0.002 superior	0.070 fair	−0.032 excellent	0.010 superior	−0.022 excellent	−0.025 excellent	0.025 excellent	0.028 excellent	0.120 poor

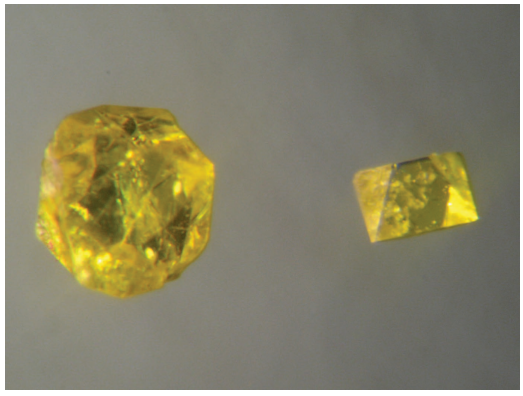

FIG. 5. Pseudo-octahedral crystals of betpakdalite-CaMg (NHMLAC 63327). The larger crystal is about 1 mm in diameter. The smaller crystal was used in the structure refinement.

refinement for any betpakdalite-group mineral. As other structure refinements for minerals of this group were much less successful in defining the non-framework sites, this refinement is considered definitive of the structure type. The structure of betpakdalite-CaMg is shown in Fig. 2. Details of the data collection and refinement are provided in Table 5. Final atom coordinates and displacement parameters are provided in Table 6, selected bond distances in Table 7, and a bond-valence analysis of the framework portion of the structure in Table 8.

Betpakdalite-NaNa (IMA2011-078) – new species

$[Na_2(H_2O)_{16}Na(H_2O)_6][Mo_8As_2Fe^{3+}_3O_{33}(OH)_4]$

Betpakdalite-NaNa occurs at the Chuquicamata mine, Antofagasta, Chile (22°17′22″S, 68°54′4″W), the type locality for 20 minerals, including this and four other members of the heteropolymolybdate family, mendozavilite-KCa (this study), obradovicite-KCu (originally obradovicite; Finney *et al*., 1986), obradovicite-NaCu (this study) and obradovicite-NaNa (this study). Chuquicamata is a porphyry copper deposit. An overview of the geology is provided by Ossandón *et al*. (2001); the mineralogy is described by Cook (1978), and Bandy (1938) remains the most comprehensive treatment of the minerals of the oxidation zone.

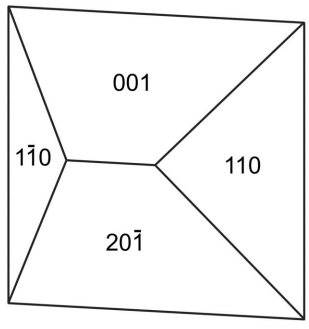

FIG. 6. Crystal drawing of betpakdalite-CaMg (clinographic projection).

Betpakdalite-NaNa is abundant on ten specimens in the collection of the Harvard Mineralogical Museum, all originally catalogued under number 95025. The specimens were received in 1940 from the Chile Exploration Company, the operator of the Chuquicamata mine, and were labelled from the "W side bench E-3 (between co-ord. N4000 & N4100 on E3330) Chuquicamata Mine". This bench exploited the upper oxidation zone, which was described by Cook (1978) as a thick blanket of oxidized waste which overlaid the zone of the strongest sulfide mineralization.

The ten specimens are split into two lots, labelled B-1 to B-5 and Y-1 to Y-5. All of the descriptive data were obtained from specimen Y-3, which is designated as the holotype; however, similar yellow crystals on all nine of the other specimens were confirmed by EMPA and EDS to be essentially identical to those on the holotype specimen and these specimens are designated as cotypes. The matrix on all of the specimens consists of brecciated vein quartz intermixed with, cemented by and/or coated with jarosite and a mixture of iron oxides and oxyhydroxides (e.g. goethite and akaganéite). Minor associated species include scorodite and topaz. Excellent crystals of leightonite, up to 1 cm long, occur on specimens B-1 to B-5. The holotype specimen (Y-3) and one cotype (B-5) have been deposited in the collections of the Natural History Museum of Los Angeles County under catalogue numbers 63570 and 63571, respectively. Sample Y-4 is now in the collections of Museum Victoria, catalogue number M51648.

Betpakdalite-NaNa is an oxidation zone mineral which is presumed to have formed as a result of the alteration of Fe, As and Mo sulfides (e.g. pyrite, arsenopyrite and molybdenite) by solutions rich in Na. It occurs as striated prismatic to bladed crystals, flattened on {001} and elongated parallel to [010], up to about 0.4 mm in length and 0.1 mm

TABLE 5. Data collection and structure refinement details for betpakdalite-CaMg and obradovicite-NaNa.

	Betpakdalite-CaMg	Obradovicite-NaNa
Diffractometer	Rigaku R-Axis Rapid II	Rigaku R-Axis Rapid II
X-ray radiation (wavelength)	Mo$K\alpha$ (λ = 0.71075 Å)	Mo$K\alpha$ (λ = 0.71075 Å)
X-ray power	50 kV, 40 mA	50 kV, 40 mA
Temperature	298(2) K	298(2) K
Space group	*C*2/*m*	*Pnmb*
Unit cell dimensions (Å/º)	*a* = 19.5336(7)	*a* = 14.8866(11)
	b = 11.0637(4)	*b* = 11.0880(2)
	c = 15.2559(11)	*c* = 15.0560(3)
	β = 131.528(9)	
V (Å^3)	2468.3(2)	2485.2(2)
Z	2	2
Density (g cm^{-3})*	2.915	2.635
Absorption coefficient (mm^{-1})*	4.502	4.254
F(000)*	2041.1	1847.2
Crystal size (μm)	400 × 240 × 200	120 × 80 × 40
θ range (º)	3.39 to 30.51	3.03 to 27.48
Index ranges	$-27 \leqslant h \leqslant 27$	$-19 \leqslant h \leqslant 19$
	$-15 \leqslant k \leqslant 15$	$-14 \leqslant k \leqslant 14$
	$-21 \leqslant l \leqslant 21$	$-19 \leqslant l \leqslant 19$
Reflections collected/unique	41,857/3927 [R_{int} = 0.0162]	28,777/2990 [R_{int} = 0.0509]
Reflections $F_o > 4\sigma F$	3880	2664
Completeness	99.7%	98.9%
Max. and min. transmission*	0.4663 and 0.2661	0.8483 and 0.6293
Refinement method	Full-matrix least-squares on F^2	Full-matrix least-squares on F^2
Parameters refined	244	186
GoF	1.219	1.090
Final *R* indices [$F_o > 4\sigma F$]	R_1 = 0.0213, wR_2 = 0.0548	R_1 = 0.0385, wR_2 = 0.1007
R indices (all data)	R_1 = 0.0217, wR_2 = 0.0550	R_1 = 0.0436, wR_2 = 0.1034
Largest diff. peak/hole (*e* A^{-3})	+1.094/−0.620	+1.732/−0.906

The SXRD refinement parameters are as follows:
$R_{int} = \Sigma|F_o^2 - F_o^2(\text{mean})|/\Sigma[F_o^2]$;
GoF = $S = \{\Sigma[w(F_o^2 - F_c^2)^2]/(n-p)\}^{1/2}$;
$R_1 = \Sigma||F_o| - |F_c||/\Sigma|F_o|$;
$wR_2 = \{\Sigma[w(F_o^2 - F_c^2)^2]/\Sigma[w(F_o^2)^2]\}^{1/2}$;
$w = 1/[\sigma^2(F_o^2) + (aP)^2 + bP]$ where P is $[2F_c^2 + \text{Max}(F_o^2,0)]/3$; for betpakdalite-CaMg a is 0.0249 and b is 9.5700; for obradovicite-NaNa a is 0.0526 and b is 17.626.
* Based on refined site occupancies

in diameter; the forms exhibited are {001}, {110}, {10$\bar{1}$} and {20$\bar{1}$} (Fig. 7). Ubiquitous multiple penetration twinning results in crystals with a prismatic aspect, elongated and striated parallel to [010], with wedge-shaped terminations; they are commonly doubly terminated (Fig. 8). Penetration twinning may also result in intersecting blades with X-shaped cross-sections (Fig. 9). The complexity of the multiple twinning made the twin law difficult to determine unambiguously, but it may correspond to reflection on {10$\bar{1}$} or 180º rotation about [10$\bar{3}$]; the same operation that describes the relationship between the betpakdalite and obradovicite structures. The physical and optical properties are listed in Tables 4*a* and 4*b*, respectively.

The PXRD pattern (Fig. 1) showed this mineral to be a member of the betpakdalite group and EMPA (Table 3*a*) showed it to be a new species corresponding to betpakdalite-NaNa with the empirical formula $[(Na_{2.86}K_{0.67})_{\Sigma 3.53}(H_2O)_{14.47}(Na_{0.90}Ca_{0.05}Cu^{2+}_{0.05})_{\Sigma 1.00}(H_2O)_6][Mo_8(As_{1.46}P_{0.31})_{\Sigma 1.77}Fe^{3+}_{2.98}O_{33.42}(OH)_{3.58}]$. The crystal structure, refined from single-crystal XRD data [R_1=

TABLE 6*a*. Atom coordinates and displacement parameters (Å^2) for betpakdalite-CaMg.

	x/*a*	*y*/*b*	*z*/*c*	U_{eq}	U_{11}	U_{22}	U_{33}	U_{23}	U_{13}	U_{12}
Mo1	0.214851(11)	−0.160513(15)	0.193999(14)	0.00835(5)	0.00993(8)	0.00816(8)	0.00875(8)	0.00072(5)	0.00695(7)	0.00080(5)
Mo2	0.370947(16)	0.0000	0.19671(2)	0.00797(5)	0.00734(10)	0.00876(10)	0.00776(10)	0.000	0.00498(9)	0.000
Mo3	0.375826(17)	0.0000	0.42469(2)	0.01243(6)	0.00946(11)	0.01899(12)	0.00823(11)	0.000	0.00560(9)	0.000
As	−0.134700(19)	0.0000	0.05865(2)	0.00844(6)	0.00817(12)	0.00905(13)	0.00843(12)	0.000	0.00564(11)	0.000
Fe1	0.7500	0.7500	0.0000	0.01106(8)	0.01247(18)	0.00966(18)	0.01233(18)	0.00073(14)	0.00876(16)	−0.00046(14)
Fe2	0.0000	0.0000	0.0000	0.01209(11)	0.0108(3)	0.0145(3)	0.0126(3)	0.000	0.0084(2)	0.000
O1	0.21258(14)	0.0000	0.09237(18)	0.0098(4)	0.0088(9)	0.0113(9)	0.0076(8)	0.000	0.0047(8)	0.000
O2	0.23791(14)	0.0000	0.28512(19)	0.0115(4)	0.0104(9)	0.0145(10)	0.0104(9)	0.000	0.0072(8)	0.000
O3	0.34240(11)	−0.12493(15)	0.10234(15)	0.0155(3)	0.0165(7)	0.0141(7)	0.0184(7)	−0.0040(6)	0.0126(6)	−0.0021(6)
O4	0.35036(10)	−0.11319(15)	0.28652(13)	0.0130(3)	0.0111(6)	0.0163(7)	0.0121(6)	0.0004(6)	0.0078(6)	0.0007(6)
O5	0.21873(12)	−0.25423(15)	0.10148(14)	0.0158(3)	0.0221(8)	0.0130(7)	0.0181(7)	−0.0017(6)	0.0158(7)	−0.0007(6)
O6	0.09475(11)	−0.12795(15)	0.10119(14)	0.0153(3)	0.0118(7)	0.0159(7)	0.0166(7)	0.0005(6)	0.0087(6)	0.0001(6)
O7	0.15162(12)	−0.12422(15)	−0.10525(14)	0.0182(3)	0.0223(8)	0.0141(7)	0.0136(7)	−0.0024(6)	0.0100(7)	0.0060(6)
O8	0.02891(15)	0.0000	−0.1055(2)	0.0177(5)	0.0090(9)	0.0306(13)	0.0141(10)	0.000	0.0079(9)	0.000
O9	0.37073(13)	−0.12265(18)	0.48874(15)	0.0231(4)	0.0222(8)	0.0241(9)	0.0146(7)	0.0027(7)	0.0086(7)	−0.0024(7)
O10	0.48694(16)	0.0000	0.2921(2)	0.0175(4)	0.0114(10)	0.0237(12)	0.0149(10)	0.000	0.0077(9)	0.000
O11	0.23494(13)	−0.26014(17)	0.29470(15)	0.0200(3)	0.0262(9)	0.0191(8)	0.0196(8)	0.0052(6)	0.0172(7)	0.0020(7)
O12	0.5000	0.0000	0.5000	0.0275(9)	0.0082(14)	0.058(3)	0.0116(15)	0.000	0.0046(13)	0.000
Mg	0.5000	0.0000	0.0000	0.0152(3)	0.0102(6)	0.0195(7)	0.0164(7)	0.000	0.0091(6)	0.000
OW1	0.46462(18)	−0.1355(3)	0.0570(2)	0.0495(7)	0.0383(13)	0.0670(19)	0.0459(14)	0.0024(13)	0.0291(12)	−0.0204(13)
OW2	0.6282(2)	0.0000	0.1656(3)	0.0389(8)	0.0215(14)	0.055(2)	0.0275(15)	0.000	0.0108(13)	0.000
Ca	0.15478(9)	−0.17861(11)	0.48479(11)	0.0292(4)	0.0292(7)	0.0241(6)	0.0287(7)	0.0101(4)	0.0169(5)	0.0001(4)
OW3	−0.2093(3)	0.0000	0.2204(3)	0.0389(8)	0.054(2)	0.0364(17)	0.049(2)	0.000	0.0432(19)	0.000
OW4	0.1270(3)	−0.0485(5)	0.3388(4)	0.0388(14)	0.033(2)	0.060(3)	0.027(2)	0.0084(18)	0.0212(19)	0.0001(19)
OW5	−0.1082(4)	−0.0282(6)	0.4607(5)	0.064(3)	0.067(4)	0.059(6)	0.056(3)	0.002(3)	0.037(3)	−0.015(3)
OW6	−0.2934(3)	−0.0430(4)	0.4060(4)	0.0372(13)	0.044(3)	0.034(2)	0.040(2)	−0.0023(17)	0.030(2)	0.0004(17)
OW7	−0.2310(4)	−0.1986(4)	0.5053(5)	0.0363(15)	0.054(3)	0.030(2)	0.047(3)	0.001(2)	0.043(3)	0.007(2)
OW8	0.4770(3)	−0.3086(4)	0.3511(7)	0.066(2)	0.055(3)	0.055(3)	0.054(4)	−0.003(2)	0.022(2)	0.008(2)
OW9	0.0569(5)	−0.2326(8)	0.2578(7)	0.058(2)	0.053(4)	0.054(5)	0.058(4)	0.003(4)	0.034(3)	0.002(3)
OW10	0.4160(7)	−0.1978(12)	0.6985(9)	0.044(4)	0.045(6)	0.051(8)	0.031(5)	−0.006(5)	0.023(4)	−0.013(5)
OW11	0.5140(17)	−0.268(2)	0.306(2)	0.069(9)						
OW12	0.4922(18)	−0.303(2)	0.412(3)	0.071(8)						

Site occupancies: Ca: Ca 0.96(8)/Na 0.04(8); OW4: 0.528(9); OW5: 0.515(9); OW6: 0.546(9); OW7: 0.495(9); OW8: 0.77(2); OW9: 0.526(16); OW10: 0.297(15); OW11: 0.157(12); OW12: 0.21(2).

TABLE 6*b*. Atom coordinates and displacement parameters (Å^2) for obradovicite-NaNa.

	x/*a*	*y*/*b*	*z*/*c*	U_{eq}	U_{11}	U_{22}	U_{33}	U_{23}	U_{13}	U_{12}
Mo1	0.20915(3)	0.65997(4)	0.47922(3)	0.01298(13)	0.0129(2)	0.0129(2)	0.0131(2)	−0.00013(16)	−0.00069(15)	−0.00106(15)
Mo2	0.33768(4)	0.5000	0.32183(4)	0.01254(15)	0.0102(3)	0.0131(3)	0.0142(3)	0.000	−0.0002(2)	0.000
Mo3	0.38399(4)	0.5000	0.54912(4)	0.01694(16)	0.0122(3)	0.0226(3)	0.0160(3)	0.000	−0.0035(2)	0.000
Fe1	0.20109(7)	0.7500	0.2500	0.0148(2)	0.0162(5)	0.0123(5)	0.0160(5)	0.0018(4)	0.000	0.000
Fe2	0.0000	0.5000	0.5000	0.0155(3)	0.0136(7)	0.0170(7)	0.0159(7)	0.000	0.0027(6)	0.000
As	0.09972(5)	0.5000	0.30715(5)	0.01216(16)	0.0114(3)	0.0120(3)	0.0130(3)	0.000	−0.0005(3)	0.000
O1	0.1907(3)	0.5000	0.3784(3)	0.0123(9)	0.010(2)	0.014(2)	0.013(2)	0.000	−0.0033(18)	0.000
O2	0.2451(3)	0.5000	0.5450(3)	0.0165(10)	0.012(2)	0.024(3)	0.014(2)	0.000	−0.0010(19)	0.000
O3	0.2978(2)	0.6247(3)	0.2571(3)	0.0179(7)	0.0189(18)	0.0152(17)	0.0195(18)	0.0031(15)	0.0003(15)	0.0023(14)
O4	0.3386(2)	0.3867(3)	0.4339(2)	0.0176(7)	0.0148(17)	0.0220(18)	0.0160(17)	0.0017(15)	−0.0004(14)	0.0001(14)
O5	0.1984(2)	0.7538(3)	0.3829(2)	0.0182(7)	0.0207(18)	0.0163(17)	0.0176(17)	0.0010(14)	0.0032(14)	0.0025(14)
O6	0.0941(2)	0.6284(3)	0.5072(3)	0.0188(8)	0.0158(17)	0.0193(18)	0.0214(19)	0.0008(16)	0.0025(14)	−0.0011(15)
O7	0.1049(2)	0.8763(4)	0.2560(3)	0.0217(8)	0.0203(18)	0.0194(18)	0.025(2)	0.0078(16)	0.0063(16)	0.0052(15)
O8	0.0056(3)	0.5000	0.3670(4)	0.0213(11)	0.014(2)	0.033(3)	0.017(3)	0.000	0.000(2)	0.000
O9	0.3895(3)	0.3782(4)	0.6178(3)	0.0336(10)	0.028(2)	0.041(3)	0.032(2)	0.014(2)	−0.0131(18)	−0.0065(19)
O10	0.4494(4)	0.5000	0.3002(4)	0.0253(12)	0.013(3)	0.040(3)	0.024(3)	0.000	0.002(2)	0.000
O11	0.2399(3)	0.7607(4)	0.5592(3)	0.0239(8)	0.026(2)	0.025(2)	0.0214(19)	−0.0060(16)	−0.0026(16)	−0.0025(17)
O12	0.5000	0.5000	0.5000	0.0272(18)	0.009(3)	0.045(5)	0.027(4)	0.000	−0.001(3)	0.000
Na1	0.0000	0.0000	0.5000	0.089(6)	0.123(12)	0.042(6)	0.103(10)	0.000	0.069(8)	0.000
OW1	0.1616(12)	0.0000	0.4423(8)	0.107(7)	0.211(18)	0.032(5)	0.077(9)	0.000	−0.042(9)	0.000
OW2	−0.0315(5)	0.1635(8)	0.3862(6)	0.097(4)	0.077(6)	0.103(7)	0.112(7)	−0.054(5)	0.047(5)	−0.018(4)
Na2A	0.272(2)	0.7500	0.7500	0.158(17)						
Na2B	0.178(3)	0.7500	0.7500	0.18(2)						
Na3A	0.1806(17)	0.0000	0.6200(7)	0.056(4)						
Na3B	0.216(3)	0.0000	0.6214(18)	0.017(13)						
OW3	0.4297(8)	0.1856(11)	0.3869(8)	0.121(6)						
OW4A	0.1634(14)	0.0000	0.7925(14)	0.054(9)						
OW4B	0.1582(14)	0.938(3)	0.7889(14)	0.044(9)						
OW5	0.360(3)	0.0000	0.479(3)	0.19(2)						
OW6	0.528(3)	0.2500	0.2500	0.13(2)						

Site occupancies: Na1: 0.76(3); OW1: 0.97(4); OW2: 1.00(3); Na2A: 0.42(4); Na2B: 0.32(4); Na3A: 0.52(4); Na3B: 0.12(4); OW3: 0.93(3); OW4A: 0.46(6); OW4B: 0.28(3); OW5: 0.60(5); OW6: 0.33(4).

TABLE 7. Selected bond distances (Å) in betpakdalite-CaMg and obradovicite-NaNa.

	Betpakdalite -CaMg	Obradovicite -NaNa	Betpakdalite-CaMg		Obradovicite-NaNa	
Mo1–O11	1.7116(17)	1.708(4)	Mg–OW2 (×2)	2.065(3)	Na1–OW1 (×2)	2.556(18)
Mo1–O5	1.7930(16)	1.794(4)	Mg–OW1 (×4)	2.068(3)	Na1–OW2 (×4)	2.543(10)
Mo1–O6	1.7983(16)	1.796(4)	<Mg–O>	2.067	<Na–O>	2.547
Mo1–O4	2.0782(15)	2.106(4)				
Mo1–O2	2.1116(12)	2.105(3)	Ca–OW5	2.300(7)	Na2A–OW4B (×2)	2.75(3)
Mo1–O1	2.3384(14)	2.355(3)	Ca–OW11	2.328(24)	Na2A–O11	2.917(7)
<Mo–O>	1.9719	1.977	Ca–O9	2.348(2)	Na2A–OW6	2.98(6)
			Ca–OW4	2.393(4)	Na2A–O9 (×2)	3.01(2)
Mo2–O10	1.697(2)	1.693(6)	Ca–OW7	2.448(5)	Na2B–OW4A (×2)	2.859(7)
Mo2–O3 (×2)	1.7971(16)	1.795(4)	Ca–OW6	2.526(5)	Na2B–O11	3.021(16)
Mo2–O4 (×2)	2.0827(16)	2.107(4)	Ca–OW10	2.544(9)	Na3A–OW4A	2.61(2)
Mo2–O1	2.361(2)	2.345(5)	Ca–OW12	2.584(21)	Na3A–OW4B (×2)	2.66(2)
<Mo–O>	1.970	1.974	Ca–O11	2.609(2)	Na3A–OW2 (×2)	2.87(2)
			Ca–OW8	2.617(5)	Na3A–O11 (×2)	2.947(9)
Mo3–O9 (×2)	1.7131(19)	1.706(5)	Ca–OW9	2.688(7)	Na3B–OW4A	2.69(4)
Mo3–O12	1.8730(3)	1.8768(14)	<Ca–O>	2.490	Na3B–OW4B (×2)	2.75(4)
Mo3–O2	2.046(2)	2.065(5)			Na3B–O11 (×2)	2.842(11)
Mo3–O4 (×2)	2.2064(16)	2.249(4)				
<Mo–O>	1.960	1.975				
Fe1–O3 (×2)	1.9681(16)	2.004(4)				
Fe1–O5 (×2)	2.0065(16)	2.005(4)				
Fe1–O7 (×2)	2.0290(16)	2.005(4)				
<Fe–O>	2.0012	2.005				
Fe2–O6 (×4)	2.0060(16)	2.001(4)				
Fe2–O8 (×2)	2.029(2)	2.007(6)				
<Fe–O>	2.014	2.003				
As–O7 (×2)	1.6777(16)	1.674(4)				
As–O8	1.680(2)	1.665(5)				
As–O1	1.725(2)	1.727(5)				
<As–O>	1.690	1.685				

0.0603 for 1435 $F_o > 4\sigma F$], shows Na to occupy the octahedrally coordinated non-framework *B* site with Na–O distances of 2.77 (×4) and 2.78 (×2) Å. This refinement is particularly significant in that it shows that cations as large as Na^+ can occupy the *B* site in the betpakdalite structure in the absence of smaller cations, such as Ca, Mg or Cu. As the structure refinement of betpakdalite-CaMg is much better at showing the other details of the betpakdalite structure type, we do not report the details of the betpakdalite-NaNa refinement here; however, a crystallographic information file has been deposited with the Editor of *Mineralogical Magazine* and can be downloaded from http://www.minersoc.org/pages/e_journals/dep_mat_mm.html.

Betpakdalite supergroup: mendozavilite group

Mendozavilite – new suffix-based name: mendozavilite-NaFe

$[Na_2(H_2O)_{15}Fe^{3+}(H_2O)_6][Mo_8P_2Fe_3^{3+}O_{35}(OH)_2]$

Mendozavilite was first described from the San Judas mine, Cumobabi, Moctezuma, Sonora, Mexico by Williams (1986). He derived an ideal formula $Na(Ca,Mg)_2[Fe_6^{3+}(PO_4)_2(PMo_{11}O_{39})(OH,Cl)_{10}]\cdot 33H_2O$ from wet chemistry. No crystal system or cell parameters were provided. The reported powder data are similar to those of betpakdalite.

Using crystals from a cotype specimen of mendozavilite at the Natural History Museum,

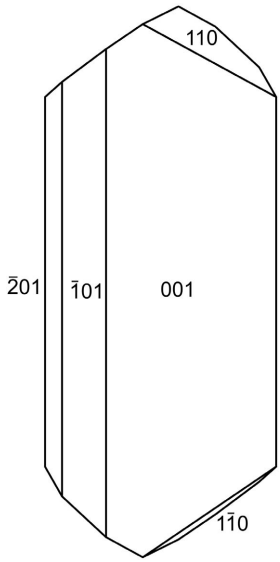

FIG. 7. Crystal drawing of an untwinned betpakdalite-NaNa crystal (clinographic projection in non-standard orientation).

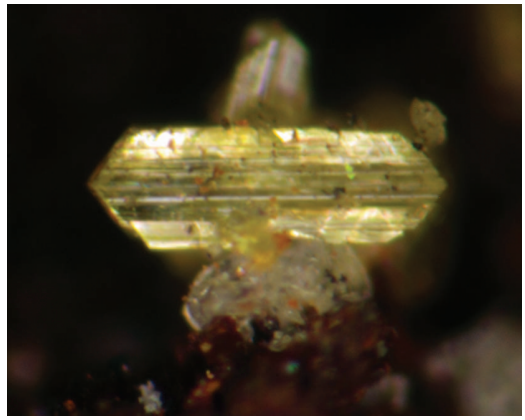

FIG. 8. Betpakdalite-NaNa crystal (0.2 mm long) on a scorodite crystal (NHMLAC 63570). Note that, although the crystal appears to be an individual, it is actually multiply twinned.

London (BM 1984,475), we recorded a PXRD pattern (Fig. 1) that is very similar to those of the other betpakdalite-group minerals. Analyses of material from the same specimen (Table 3*b*) show significant differences from the analysis reported by Williams (1986). In particular, the new analysis contains more MoO_3, CaO, and Na_2O, and includes K_2O, which was not reported by Williams (1986). The empirical formula based on our EMPA, $[(Na_{1.22}K_{1.14}Ca_{1.01})_{\Sigma 3.37}(H_2O)_{13.63}(Fe^{3+}_{0.53}Ca_{0.44}Cu^{2+}_{0.03})_{\Sigma 1.00}(H_2O)_6][Mo_{7.77}(P_{1.95}Si_{0.05})_{\Sigma 2.00}(Fe^{3+}_{2.85},Al_{0.15})_{\Sigma 3.00}O_{31.62}(OH)_{5.29}Cl_{0.09}]$, corresponds to

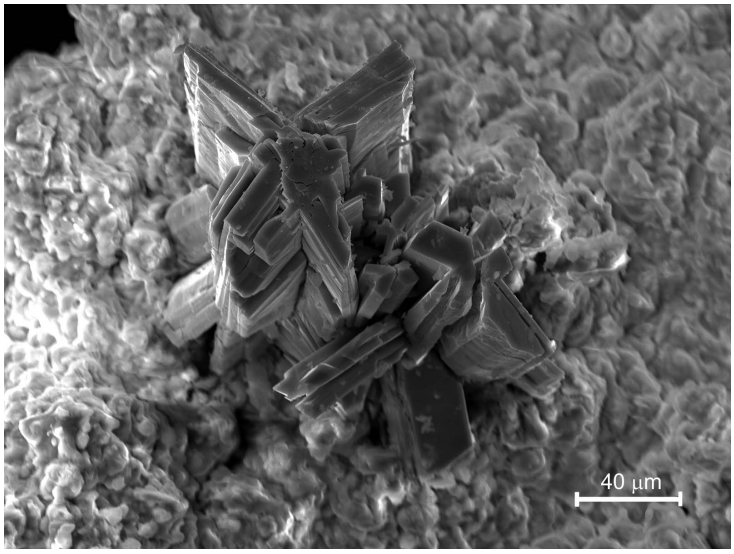

FIG. 9. Scanning electron microscope image of twinned crystals of betpakdalite-NaNa (fragment from NHMLAC 63571).

mendozavilite-NaFe, whereas the original analysis corresponded to *mendozavilite-CaFe*. We consider our analysis to be more reliable and, therefore, identify the original mendozavilite as mendozavilite-NaFe. It is possible that compositions corresponding to *mendozavilite-CaFe* occur at the San Judas mine or elsewhere, but this name should not be considered valid until such a composition is confirmed and described.

In the course of this project, we identified a dark brown massive mineral corresponding to mendozavilite-NaFe, which is much richer in Fe than the mendozavilite cotype, in association with mendozavilite-NaCu at the Lomas Bayas mine, 93 km ENE of Antofagasta, Antofagasta Province, Chile (see below). The EMPA (Table 3*b*) provided an empirical formula $[(Na_{0.70}Mg_{0.52}Fe^{3+}_{0.51}K_{0.10}Ca_{0.02}Cu^{2+}_{0.01}Al_{0.01})_{\Sigma 1.87}(H_2O)_{15.13}Fe^{3+}(H_2O)_6][Mo_8P_{1.81}Fe^{3+}_3O_{35.52}(OH)_{1.48}]$ for this material.

Melkovite – existing name is retained instead of mendozavilite-CaCa

$[Ca_2(H_2O)_{15}Ca(H_2O)_6][Mo_8P_2Fe^{3+}_3O_{36}(OH)]$

Melkovite was first described by Yegorov *et al.* (1969) from a U-Mo deposit in the Shunak mountains, 60 km west of the Mointy railroad station, Kazakhstan. The name honours Professor Vyacheslav Gavrilovich Melkov (1911–1991), a Russian mineralogist who specialized in uranium minerals. The original publication did not provide information on the crystal system or unit cell, but noted a probably close relationship between melkovite and betpakdalite based on similarities in their occurrences, chemistries and PXRD patterns.

A cotype specimen of melkovite from the Smithsonian Institution (NMNH 160237) did not provide crystals suitable for single-crystal work; however, the PXRD pattern (Fig. 1) obtained from that material confirms the close match with the PXRD patterns of other betpakdalite supergroup species. Our EMPA (Table 3*b*) on this cotype material is reasonably close to that reported in the original description and provides the empirical formula $[(Ca_{1.27}Na_{0.51}K_{0.07}Cu^{2+}_{0.02})_{\Sigma 1.87}(H_2O)_{15.13}Ca(H_2O)_6][Mo_8(P_{1.74}As_{0.01}Si_{0.06})_{\Sigma 1.83}Fe^{3+}_{2.68}O_{33.17}(OH)_{3.83}]$, corresponding to 'mendozavilite-CaCa'.

Birch *et al.* (2002) described "mendozavilite" from the Fitzgerald River district, Western Australia. Their EMPA analysis (Table 3*b*) provides the empirical formula $[(Ca_{0.87}Na_{0.64}K_{0.14}Sr_{0.06})_{\Sigma 1.71}(H_2O)_{15.29}(Ca_{0.81}Mg_{0.19})_{\Sigma 1.00}(H_2O)_6][Mo_8P_{2.00}Fe^{3+}_{2.98}O_{34.58}(OH)_{2.42}]$ corresponding to melkovite, but relatively close to *mendozavilite-NaCa*, which would be a new species. A mendozavilite-group mineral with a composition corresponding to melkovite occurs at Su Senargiu, Sardinia, Italy (Paolo Orlandi, pers. comm.).

Mendozavilite-NaCu (IMA2011-039) – new species

$[Na_2(H_2O)_{15}Cu^{2+}(H_2O)_6][Mo_8P_2Fe^{3+}_3O_{34}(OH)_3]$

Mendozavilite-NaCu occurs at the Lomas Bayas mine, 93 km ENE of Antofagasta, Antofagasta Province, Chile (23º25′40″S, 69º30′41″W), as thin vein fillings and well formed crystals in cavities in a matrix of quartz with feruvite, muscovite (sericite) and massive sulfides including pyrite, chalcopyrite, covellite, djurleite and molybdenite. Associated secondary minerals include anhydrite, jarosite, mendozavilite-NaFe, natrochalcite, sampleite and strengite. The Lomas Bayas mine is a porphyry copper deposit and the new mineral occurs in the oxidation zone. It is presumed to have resulted from the alteration of Cu, Fe and Mo sulfides by solutions rich in Na and P. A general description of the deposit is provided by Shrake *et al.* (1996). Four cotype specimens, all collected by one of the authors (RAJ), are deposited in the collections of the Natural History Museum of Los Angeles County, under catalogue numbers 60483, 60484, 60485 and 60486.

Mendozavilite-NaCu occurs as lime-green six-sided (pseudohexagonal) tabular crystals up to 1 mm across and 0.1 mm thick (Fig. 10). Forms exhibited are {001} (dominant), {110}, {111}, {20$\bar{1}$} and {110} (Fig. 11). Twinning is ubiquitous: contact on {001} and penetration, both by rotation of 120º about [102]. The physical and optical properties are listed in Tables 4*a* and 4*b*, respectively.

The PXRD pattern (Fig. 1) showed this mineral to be a member of the mendozavilite group and EMPA (Table 3*b*) showed it to be a new species corresponding to mendozavilite-NaCu. The H_2O content was determined by CHN analysis on 1.8 and 2.1 mg samples, yielding 15.19 wt.% H_2O; however, because of the difficulty of separating pure samples and the small sample sizes, we consider the density determined on a Berman balance to be a more reliable basis for determination of the H_2O content. The empirical formula

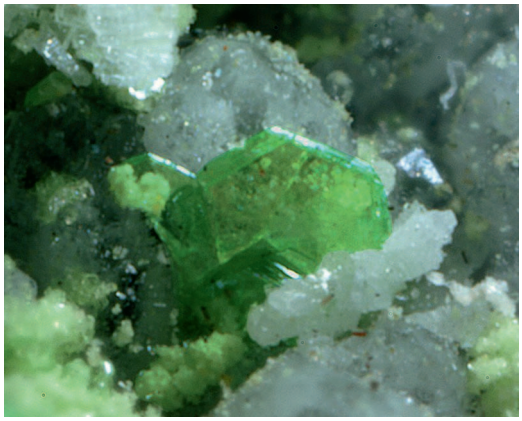

FIG. 10. Crystals of mendozavilite-NaCu on quartz (NHMLAC 60483). The largest crystal is about 1 mm across.

(based on Mo = 8) is $[(Na_{1.61}Mg_{0.27}Ca_{0.04}K_{0.03}Cu^{2+}_{0.07})_{\Sigma 2.02}(H_2O)_{13.39}Cu^{2+}(H_2O)_6][Mo_8(P_{1.87}Si_{0.01})_{\Sigma 1.88}(Fe^{3+}_{2.83}Al_{0.01})_{\Sigma 2.84}O_{33.31}(OH)_{3.69}]$.

Structure data [R_1 = 0.0596 for 2185 $F_o > 4\sigma F$] were collected at ChemMatCARS, Sector 15, Advanced Photon Source at Argonne National Laboratory, USA. The framework is the same as that of betpakdalite, but with P replacing As (Cooper and Hawthorne 1999). Open space within the framework is occupied by a $Cu^{2+}(H_2O)_6$ octahedron at [½;0;0] and disordered Na atoms and H_2O molecules. The framework atoms refine very well at full occupancy; however, all non-framework atom positions are fractionally occupied and significant additional electron density is distributed throughout the open space, indicating considerable disorder. It is difficult in some cases to determine unambiguously whether non-framework sites are occupied by Na or H_2O. The Cu^{2+} at the [½;0;0] site exhibits low occupancy and essentially holosymmetric coordination with Cu–O distances of 2.242 (×2) and 2.299 (×4) Å. This sort of Cu^{2+} coordination is due to orientational averaging of the Jahn–Teller distortion (Burns and Hawthorne, 1996). As the structure refinement for betpakdalite-CaMg shows the other details of the betpakdalite structure type, we have not included further details of our mendozavilite-NaCu refinement here; a crystallographic information file for this refinement has been deposited with the Editor of *Mineralogical Magazine* and can be downloaded from http://www.minersoc.org/pages/e_journals/dep_mat_mm.html.

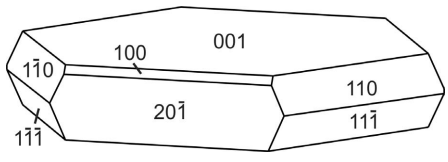

FIG. 11. Crystal drawing of an untwinned mendozavilite-NaCu crystal (clinographic projection).

Mendozavilite-KCa (IMA2011-088) – new species

$[K_2(H_2O)_{15}Ca(H_2O)_6][Mo_8P_2Fe^{3+}_3O_{34}(OH)_3]$

Mendozavilite-KCa occurs on massive vein quartz associated with jarosite on two cotype specimens (see below) collected from the dumps of the Chuquicamata mine by former mine engineer Ramn Tabilo (see the betpakdalite-NaNa subsection for further details of this locality). The precise location where the specimen was collected is not known; however, the chemistry and mineral associations are consistent with the upper C to E benches in the northwest portion of the deposit. These benches exploited the upper oxidation zone described by Cook (1978) as a thick blanket of oxidized waste which overlaid the zone of the strongest sulfide mineralization. Phases fitting at least three general mendozavilite compositions were noted on the larger of the cotype specimens (63572). Greenish yellow pseudohexagonal tabular crystals, which are distinctly richer in K than Na, correspond to mendozavilite-KCa. Yellowish green densely packed crystal intergrowths which contain almost equal amounts of K and Na, have some areas which are slightly more Na-rich, but not sufficiently so to be statistically significant and to warrant the description of the new mineral *mendozavilite-NaCa*. A few small areas of bright lime-green material have a composition consistent with mendozavilite-NaCu. Mendozavilite-KCa is an oxidation zone mineral which is presumed to have been formed as a result of the alteration of Fe, Cu and Mo sulfides (e.g. pyrite, chalcopyrite and molybdenite) by solutions rich in K, Ca and P. The two cotype specimens described above have been deposited in the collections of the Natural History Museum of Los Angeles County, Los Angeles, California, USA under catalogue numbers 63315 and 63572. A microprobe mount containing material removed from 63572 has been deposited

in the collections of the Natural History Museum, London, catalogue number BM 2011,150.

The mineral occurs as greenish yellow, six-sided (pseudohexagonal), tabular crystals up to 0.5 mm across and 0.05 mm thick (Fig. 12). The crystals are usually tightly intergrown in compact veinlets and coatings. The morphology and twinning are essentially identical to those of mendozavilite-NaCu. The forms exhibited are {001} (dominant), {110}, {111}, {20$\bar{1}$}, and {110} (Fig. 11). Penetration and contact twinning is ubiquitous: contact on {001} and penetration, both by rotation of 120º about [102]. The physical and optical properties are listed in Tables 4*a* and 4*b*, respectively.

The PXRD pattern (Fig. 1) showed this mineral to be a member of the mendozavilite group and EMPA (Table 3*b*) showed it to be a new species corresponding to mendozavilite-KCa. The H_2O determined by CHN analysis on a 3.4 mg sample yielded 12.15 wt.% H_2O; however, the sample mostly consisted of the yellowish green mendozavilite phase with roughly equal amounts of K and Na and unavoidably also included less hydrated impurities. We believe that the H_2O content obtained from the CHN analysis is significantly lower than the actual water content of mendozavilite-KCa. In this instance, we have chosen to use an H_2O content based on the measured density. The empirical formula (based on Mo = 8) is $[(K_{1.43}Na_{1.12}Ca_{0.14})_{\Sigma 2.69}(H_2O)_{9.02}(Ca_{0.94}Cu^{2+}_{0.05}Al_{0.01})_{\Sigma 1.00}(H_2O)_6][Mo_8(P_{1.86}As_{0.06}Si_{0.01})_{\Sigma 1.93}Fe^{3+}_{3.00}O_{34.48}(OH)_{2.52}]$.

The poor quality and ubiquitous twinning of the crystals did not permit an accurate refinement of the structure of mendozavilite-KCa [R_1 = 0.24 for 1211 $F_o > 4\sigma F$]. In spite of the high R factor, the refinement confirmed that mendozavilite-KCa has the same framework as the other mendozavilite- and betpakdalite-group minerals.

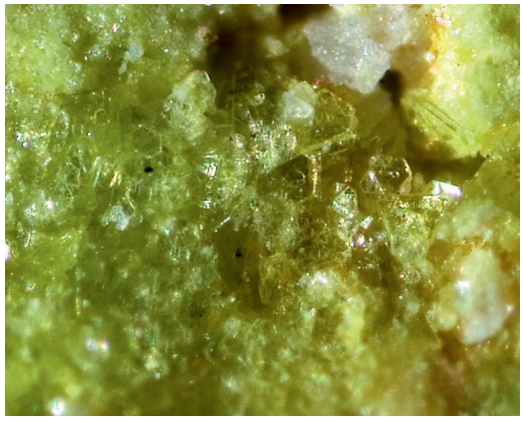

FIG. 12. Mendozavilite-KCa crystals with quartz (NHMLAC 63572). The image is 2 mm across.

Obradovicite group

Obradovicite – new suffix-based name: obradovicite-KCu

$[K_2(H_2O)_{17}Cu^{2+}(H_2O)_6][Mo_8As_2Fe^{3+}_3O_{34}(OH)_3]$

Obradovicite was described by Finney *et al.* (1986) from Chuquicamata, Chile. They reported a wet chemical analysis (Table 3*c*) from which they derived the empirical formula $H_4(K_{0.71}Na_{0.24})Cu^{2+}_{0.99}Fe^{3+}_{1.77}As_{0.99}Mo_{5.17}O_{24}\cdot 11.6H_2O$ and the ideal formula $H_4(K,Na)Cu^{2+}Fe^{3+}_2(AsO_4)(MoO_4)_5\cdot 12H_2O$. They commented on the similarity of the chemistry of obradovicite and betpakdalite (now betpakdalite-CaCa) and sodium betpakdalite (now betpakdalite-NaCa), except for the essential K and Cu in obradovicite, but they also noted a very different unit cell based on a precession X-ray study: *Pcnm*, a = 15.046, b = 14.848, c = 11.056Å and Z = 4.

As noted above, we obtained crystals from the type specimen, which is in the collection of the Colorado School of Mines Museum (CSM 86-496). It is not clear whether this specimen should be regarded as the holotype or a cotype specimen. Finney *et al.* (1986) state "The type specimen of obradovicite is preserved at the Colorado School of Mines Museum and a portion of this material will be on file with the Smithsonian Institution, Washington, DC." Both institutions have specimens of obradovicite which are classified simply as types; however, the statement by Finney *et al.* (1986) makes it clear that their description was based on material from CSM 86-496. Using crystals from this specimen, we recorded a new powder pattern and obtained a structure determination. We confirmed the space group and cell reported by Finney *et al.* (1986) and showed the obradovicite structure to be related to that of betpakdalite. The wet chemical analysis of Finney *et al.* (1986) (Table 3*c*) does not fit very well with the obradovicite-supergroup formula (which is based on the structure). Recasting the empirical formula of Finney *et al.* (1986) using our procedure yields $[(K_{1.72}Cu^{2+}_{0.58}Na_{0.38})_{\Sigma 2.68}(H_2O)_{12.25}Cu^{2+}(H_2O)_6][Mo_8As_{1.53}Fe^{3+}_{2.64}O_{31.11}(OH)_{5.89}]$. The most serious problem here is the Mo:As:Fe ratio, which is 8:1.53:2.64, rather than the ideal 8:2:3. Our EMPA data (Table 3*c*) on

material from the obradovicite type specimen indicated a composition consistent with obradovicite-NaCu, whereas the analyses reported by Finney *et al.* (1986) fits obradovicite-KCu. As the grains from the type specimen that we analysed are only slightly richer in Na than K, it seems likely that both obradovicite-NaCu and obradovicite-KCu are present on the type specimen. The occurrence of obradovicite-KCu at Chuquicamata is further indicated by EDS anlyses of a sample collected by Arturo Molina and EMP analyses of material in the collections of Museum Victoria (specimen number M51338), which fall slightly on either side of the boundary between obradovicite-NaCu and obradovicite-KCu. Obradovicite-KCu (confirmed by PXRD and EDS) from the Port Darwin mining district, Northern Territory, Australia, has also been found on a specimen dated September 1913 in the collection of the Royal Ontario Museum (K. Tait and M. Back, pers. comm.). Obradovicite-NaCu is described as a new mineral in the next subsection.

Obradovicite-NaCu (IMA2011-079) – new species

$[Na_2(H_2O)_{17}Cu^{2+}(H_2O)_6][Mo_8As_2Fe^{3+}_3O_{34}(OH)_3]$

As noted above, obradovicite-NaCu occurs on the type specimen of obradovicite (obradovicite-KCu) from the Chuquicamata mine, Antofagasta, Chile (CSM 86-496). Obradovicite-NaCu and obradovicite-KCu occur in sugary aggregates intermixed with fragmented quartz crystals embedded in a porous boxwork of hematite and goethite (Fig. 13). Finney *et al*. (1986) did not report a precise location in the mine for the original obradovicite, but the chemistry and the mineral association is consistent with the upper C to E benches in the northwest portion of the deposit, which were described by Cook (1978). Obradovicite-NaCu is an oxidation zone mineral which is presumed to have formed as a result of the alteration of Fe, Cu, As and Mo sulfides (e.g. pyrite, chalcopyrite, arsenopyrite and molybdenite) by solutions rich in Na.

The sugary aggregates consist of yellowish green short bladed crystals, flattened on {001} and elongated parallel to [010], up to ~0.1 mm in length (Figs 14 and 15). The forms observed are {001}, {110} and {101} with the {001} faces exhibiting striations parallel to [010]. Crystals are typically double terminated. No twinning was observed. The physical and optical properties are listed in Tables 4*a* and 4*b*, respectively.

The PXRD pattern (Fig. 1) showed this mineral to be a member of the obradovicite group and EMPA (Table 3*c*) showed it to be a new species corresponding to obradovicite-NaCu with the empirical formula (based on Mo = 8): $[(Na_{1.99}K_{1.72})_{\Sigma 3.71}(H_2O)_{15.29}(Cu^{2+}_{0.58}Fe^{3+}_{0.23}Na_{0.13}Ca_{0.06})_{\Sigma 1.00}(H_2O)_6][Mo_8(As_{1.77}P_{0.07}Si_{0.01})_{\Sigma 1.85}Fe^{3+}_{3.00}O_{35.05}(OH)_{1.95}]$.

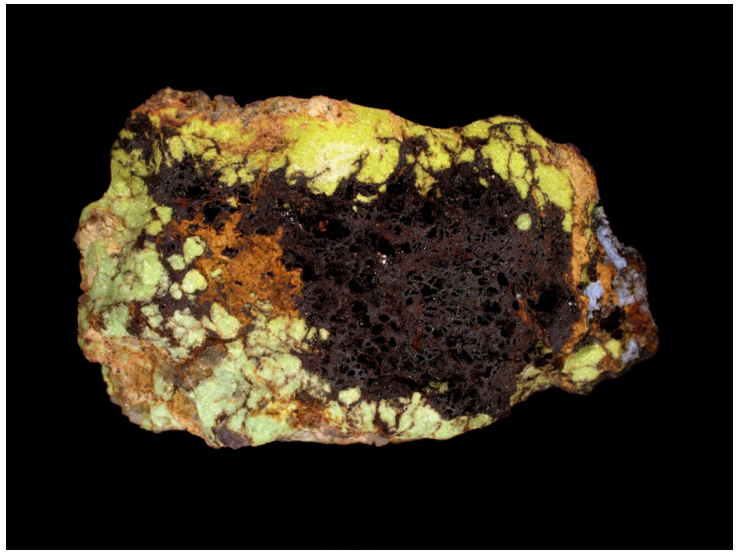

FIG. 13. Type specimen (1.8 cm across) of obradovicite-KCu and obradovicite-NaCu (CSM 86-496).

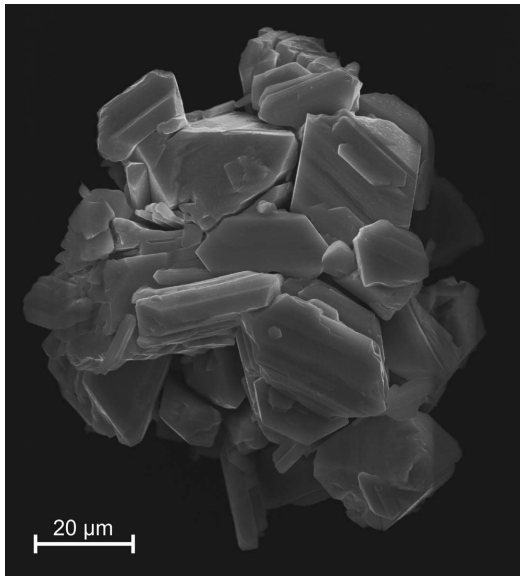

FIG. 14. SEM image of intergrown obradovicite-NaCu crystals (fragment from CSM 86-496).

The crystal structure of obradovicite was first solved using a crystal of obradovicite-NaCu [R_1= 0.0730 for 587 reflections with $F_o > 4\sigma F$]. Unfortunately, the small size and relatively poor quality of the crystal did not allow the non-framework sites to be adequately determined. However, it is noteworthy that Cu exhibits low occupancy at the [0;0;½] site and holosymmetric, rather than Jahn–Teller distorted, octahedral coordination, similar to the situation for Cu in the mendozavilite-NaCu structure. As the structure refinement for obradovicite-NaNa shows details of the obradovicite structure type far better, we do not include further details of our obradovicite-NaCu structure refinement here; a crystallographic information file for this refinement has been deposited with the Editor of *Mineralogical Magazine* and can be downloaded from http://www.minersoc.org/pages/e_journals/dep_mat_mm.html.

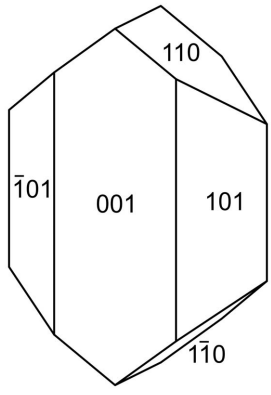

FIG. 15. Crystal drawing of obradovicite-NaCu (clinographic projection in non-standard orientation).

Obradovicite-NaNa (IMA-2011-046) – new species

$[Na_2(H_2O)_{16}Na(H_2O)_6][Mo_8As_2Fe^{3+}_3O_{33}(OH)_4]$

Obradovicite-NaNa occurs at the Chuquicamata mine, Antofagasta, Chile. Two cotype specimens, collected from the dumps of the Chuquicamata mine by former mine engineer Ramn Tabilo, have been deposited in the collections of the Natural History Museum of Los Angeles County, Los Angeles, USA, under catalogue numbers 63313 and 63314. The mineral occurs as a greenish yellow granular crystalline coating (Fig. 16) on massive quartz-muscovite rock with minor blebs of rutile. Secondary minerals in direct association include jarosite, gypsum, blödite and atacamite. The precise location where the type specimens were collected is not known; however, the chemistry and the mineral associations are consistent with the upper C to E benches in the northwest portion of the deposit (Cook, 1978). Obradovicite-NaNa is an oxidation zone mineral which is presumed to have formed as a result of the alteration of Fe, As and

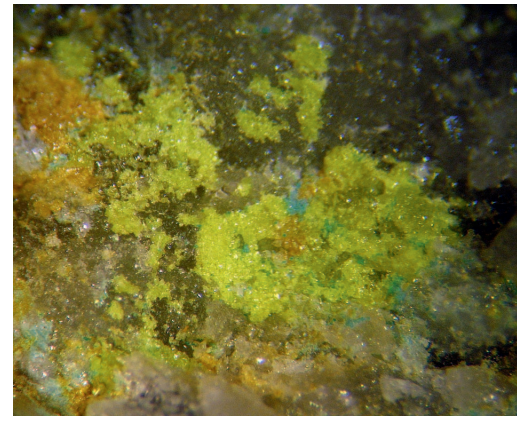

FIG. 16. Obradovicite-NaNa (yellow-green) with blue-green atacamite and orange-brown jarosite on quartz (NHMLAC 63314). The image is 5 mm across.

Mo sulfides (e.g. pyrite, arsenopyrite and molybdenite) by solutions rich in Na.

Crystals of obradovicite-NaNa are virtually identical to those of obradovicite-NaCu described above, and are up to about 0.15 mm in length. The physical and optical properties are listed in Tables 4*a* and 4*b*, respectively.

The PXRD pattern (Fig. 1) showed this mineral to be a member of the obradovicite group and EMPA (Table 3*c*) showed it to be a new species corresponding to obradovicite-NaNa. The empirical formula (based on Mo = 8) is $[(Na_{2.20}K_{1.60})_{\Sigma 3.80}(H_2O)_{14.20}(Na_{0.85}Cu^{2+}_{0.11}Ca_{0.03}Zn_{0.01})_{\Sigma 1.00}(H_2O)_6][Mo_8(As_{1.81}P_{0.05})_{\Sigma 1.86}Fe^{3+}_{2.97}O_{34.16}(OH)_{2.84}]$. Single-crystal data yielded a much better structure refinement [R_1= 0.0393 for 2670 $F_o > 4\sigma F$] than the one obtained for obradovicite-NaCu. The non-framework *B* site is clearly occupied by Na and there are at least eight channel sites partially occupied by Na/K and H_2O. The structure is shown in Fig. 2. Details of the data collection and structure refinement are provided in Table 5. Final atom coordinates and displacement parameters are provided in Table 6, selected bond distances in Table 7, and a bond-valence analysis of the framework portion of the structure in Table 8.

Other heteropolymolybdates

Paramendozavilite
$[KAl_4(H_2O)_{30}][Mo_{12}P_6Fe^{3+}_6O_{60}(OH)_{13}]$ (hypothetical)

Paramendozavilite was first described from the San Judas mine, Cumobabi, Moctezuma, Sonora, Mexico by Williams (1986). He derived the ideal formula $NaAl_4[Fe^{3+}_7(PO_4)_5(PMo_{12}O_{40})(OH)_{16}]\cdot 56H_2O$ from micro wet chemical analyses (Table 3*c*). No crystal system or cell parameters were provided.

Williams (1986) noted that a type specimen of paramendozavilite had been given to the British Museum of Natural History. Careful examination of that specimen (BM 1984,476) revealed no mineral with a powder pattern that was consistent with the published powder data for paramendozavilite. The crystals apparently mistaken for paramendozavilite on this specimen are likely to be an undescribed molybdophosphate (see below). Material on two other specimens of paramendozavilite (BM 1983,118 and NHMLAC 60464), are henceforth considered to be neotypes as they provided patterns consistent with published powder data for paramendozavilite, although EMPA (Table 3*c*) shows both of them to be K rather than Na dominant. Given the dominance of K over Na in our analyses, it seems unlikely that the material analysed by Williams contained no K; therefore, we believe that his analysis is suspect. Note also that the paramendozavilite-like species found on the supposed type paramendozavilite specimen is also K dominant and, rather surprisingly, contains no detectable Na. If Na-dominant paramendozavilite is confirmed, a suffix-based nomenclature could be used in which the Na-dominant species is named paramendozavilite-Na and the K-dominant species is named paramendozavilite-K or alternatively, if structural evidence shows that Al occupies a non-framework site, a double-suffix-based nomenclature analogous to that for the betpakdalite, mendozavilite and obradovicite groups could be employed: paramendozavilite-NaAl and paramendozavilite-KAl.

The paramendozavilite powder pattern is quite different from those of the betpakdalite- and obradovicite-group minerals (Fig. 1). Crystals of paramendozavilite are twinned and too small for structure determination; however, a twinned crystal from NHMLAC 60464 yielded a primitive monoclinic unit cell, the parameters of which were refined using the PXRD data to obtain: a = 10.963(2), b = 25.881(3), c = 15.434(2) Å and β = 110.73(1)º (Table 2). The similar chemistry and close association of paramendozavilite with mendozavilite makes it very likely that it contains a heteropolymolybdate structural unit. Similarities between the cell dimensions of mendozavilite and paramendozavilite provide further evidence for a structural relationship. Assuming that the framework cations are Mo^{6+}, P^{5+} and Fe^{3+}, their ratios suggest a somewhat different framework unit. In the absence of direct structural evidence, we suggest $[Mo_{12}P_6Fe^{3+}_6O_{59+x}(OH)_{14-x}]$ as that also is consistent with close to a whole-number (4) of $Al^{3+}(+Ti^{4+})$ and allows for charge balance with only cations and H_2O in the channels.

Unfortunately, we found it impossible to derive a reasonable ideal or empirical formula that was consistent with the H_2O content and density reported by Williams (1986). The empirical formula based on our EMPA analysis with the H_2O from Williams (1986) is $[(K_{0.54}Mg_{0.12}Ca_{0.10}Na_{0.09})_{\Sigma 0.85}(Al_{3.83}Ti_{0.13})_{\Sigma 3.96}(H_2O)_{54.20}][Mo_{12}P_{5.58}(Fe^{3+}_{5.89}Al_{0.11})_{\Sigma 6.00}O_{57.99}(OH)_{14.85}Cl_{0.16}]$. For the unit cell noted above and Z = 2, this empirical formula provides a calculated density of 3.209 g cm^{-3}, which is reasonably

TABLE 8. Bond-valence analyses for the betpakdalite-CaMg and obradovicite-NaNa frameworks. Only cations and anions in the framework are included. Values are expressed in valence units.

	O1	O2	O3	O4	O5	O6	O7	O8	O9	O10	O11	O12	Σ
Betpakdalite-CaMg													
Mo1	0.31 × 2↓	0.58 × 2↓		0.63	1.36	1.34					1.69		5.91
Mo2	0.29		1.35 × 2→	0.62 × 2→						1.76			5.99
Mo3		0.69		0.45 × 2→					1.69 × 2→			1.10 × 2↓	6.05
Fe1			0.57 × 2→		0.51 × 2→		0.48 × 2→						3.12
Fe2						0.51 × 4→		0.48 × 2→					3.02
As	1.12						1.27 × 2→	1.27					4.93
Σ	2.03	1.85	1.92	1.70	1.87	1.85	1.75	1.75	1.69	1.76	1.69	2.20	
Obradovicite-NaNa													
Mo1	0.30 × 2↓	0.59 × 2↓		0.58	1.36	1.35					1.71		5.89
Mo2	0.31		1.35 × 2→	0.58 × 2→						1.78			5.96
Mo3		0.65		0.40 × 2→					1.72 × 2→			1.08 × 2↓	5.97
Fe1			0.52 × 2→		0.51 × 2→		0.51 × 2→						3.09
Fe2						0.52 × 4→		0.51 × 2→					3.10
As	1.11						1.29 × 2→	1.32					5.00
Σ	2.02	1.83	1.87	1.56	1.87	1.87	1.80	1.83	1.72	1.78	1.71	2.16	

Multiplicity is indicated by × →↓; Mo^{6+}–O, Fe^{3+}–O and As^{5+}–O bond strengths are from Brown and Altermatt (1985).

close to the measured density of 3.35 g cm^{-3} reported by Williams (1986); however, the packing of oxygen atoms and large cations required for this cell content is close to the theoretical maximum for a close-packed structure. A rough approximation of the overall packing efficiency in these structures can be obtained by multiplying the total number of O atoms and large cations in the unit cell by the ionic volume of O (~11.5 $Å^3$) and dividing by the volume of the unit cell. For the ideal formula of mendozavilite-NaFe, the overall packing efficiency is (120 × 11.5 $Å^3$)/2421 $Å^3$ = 0.570. For the empirical formula of paramendozavilite above, the packing efficiency is (255.73 × 11.5 $Å^3$)/4095.8 $Å^3$ = 0.718, compared to the theoretical maximum packing efficiency for a close-packed structure of 0.740. Clearly, this is highly improbable for a framework structure with channels occupied by disordered cations and H_2O molecules and, furthermore, the problem cannot be solved by choosing a smaller cell content, as that lowers the density.

Consequently, we are forced to disregard the density and H_2O content reported by Williams (1986) in deriving a hypothetical ideal formula for paramendozavilite. Instead, we propose a total H_2O and large cation content of 31 p.f.u. in the channels, which yields the ideal formula $[KAl_4(H_2O)_{30}][Mo_{12}P_6Fe^{3+}_6O_{60}(OH)_{13}]$ and the empirical formula $[(K_{0.54}Mg_{0.12}Ca_{0.10}Na_{0.09})_{\Sigma 0.85}(Al_{3.83}Ti_{0.13})_{\Sigma 3.96}(H_2O)_{30.15}][Mo_{12}P_{5.58}(Fe^{3+}_{5.89}Al_{0.11})_{\Sigma 6.00}O_{57.99}(OH)_{14.85}Cl_{0.16}]$. This ideal formula yields an overall packing efficiency of (208 × 11.5 $Å^3$)/4095.8 $Å^3$ = 0.584. The calculated densities are 2.870 and 2.858 gm cm^{-3} for the ideal and empirical formulas, respectively. These values are comparable to those for the other heteropolymolybdates.

Unnamed mineral related to paramendozavilite – potential new species

The crystals mistaken for paramendozavilite on the original type specimen (BM 1984,476) provide a PXRD pattern (Fig. 1) distinct from those of paramendozavilite and all other heteropolymolybdates. The crystals are too small and imperfect to produce structure data; however, single-crystal XRD did permit the determination of a monoclinic unit cell, from which the PXRD data can be indexed. The cell parameters refined from the PXRD data are: a = 10.936(6), b = 26.28(3), c = 13.17(2) Å and β = 114.74(8)º (Table 2).

The EMPA for this phase (Table 3*c*) is very similar to that which we obtained for paramendozavilite. The chemistry, mode of occurrence and similarities in cell parameters to those of mendozavilite and paramendozavilite suggest that this phase is very likely to possess a heteropolymolybdate structural unit. Although it is quite clear that this phase is distinct from paramendozavilite and from any other known mineral, the complexity of its chemistry and the lack of specific knowledge about its structure, coupled with the poor quality of existing crystals and the small amount of material available, have stymied our efforts to adequately characterize it. We hope that more and better material will become available in the future or that improvements in technology will make its characterization possible.

Conclusions

The minerals classified as heteropolymolybdates (Table 1) possess (or are assumed to possess) structures based on infinite heteropolymolybdate frameworks. Two closely related structure types, betpakdalite and obradovicite, have thus far been recognized and both have frameworks composed of four-member clusters of edge-sharing MoO_6 octahedra linked by $Fe^{3+}O_6$ octahedra and PO_4 or AsO_4 tetrahedra. The betpakdalite, mendozavilite and obradovicite groups contain four arsenates with the betpakdalite structure, four phosphates with the betpakdalite structure and three arsenates with the obradovicite structure, respectively, the individual members being discriminated by the two types of non-framework cations in each species. A fourth group consisting of phosphates with the obradovicite structure appears feasible; however, no members have thus far been found. The structure of the molybdophosphate paramendozavilite has not been determined, but the species is assumed to possess a heteropolymolybdate framework based on its composition and association with mendozavilite-NaFe. Another phase closely related to paramendozavilite awaits characterization and, considering the variety of cations that can be accommodated in the channels of the betpakdalite and obradovicite frameworks, numerous additional members of the betpakdalite, mendozavilite, obradovicite and *phosphate-obradovicite* groups are possible.

Finally, it is worth reiterating that the term 'heteropolymolybdate' in the field of coordination chemistry generally refers to compounds whose structures contain insular clusters, rather than

frameworks. It is certainly possible that such compounds will be found in Nature. If they are, we suggest that they could be classified into a separate *insular heteropolymolybdate family*, and that the heteropolymolybdate family described herein could be renamed the *framework heteropolymolybdate family*.

Acknowledgements

Carl Francis provided specimens of betpakdalite-NaNa from the collections of the Harvard Mineralogical Museum. Dmitriy Belakovskiy provided type specimens of betpakdalite-CaCa and betpakdalite-NaCa from the collections of the Fersman Mineralogical Museum. Paul Powhat provided the cotype specimen of melkovite from the collections of the U.S. Museum of Natural History (Smithsonian Institution). Ed Raines provided the type specimen of obradovicite-KCu (and obradovicite-NaCu) from the collections of the Colorado School of Mines. Tomas Husdal provided a specimen of betpakdalite-CaCa from the Nedre Kvartsen quarry, Norway. Joe Marty provided a specimen of betpakdalite-CaCa from the Rustler mine, Utah. Jaroslav Hyršl provided specimens of betpakdalite-CaCa from Bajan Cogto, Mongolia. Arturo Molina, Richard Thomssen and Brent Thorne also provided specimens for study. Jochen Schlüter provided the results of his studies of a mendozavilite specimen from Chuquicamata, Chile, and a betpakdalite specimen from the Descubridora mine, Chile. Uwe Kolitsch provided details of his refinement of the structure of betpakdalite from Tsumeb. Kimberly Tait and Malcolm Back provided information on the specimen of obradovicite-KCu from the Port Darwin mining district, Australia. Paolo Orlandi provided information on a possible melkovite from Su Senargiu, Sardinia, Italy. Giovanni Ferraris provided comments on possible twin laws for betpakdalite-NaNa. The structure data collection for mendozavilite-NaCu was carried out at GSECARS and ChemMatCARS (CARS = Consortium for Advanced Radiation Sources) sectors 13 and 15, Advanced Photon Source at Argonne National Laboratory, with the support of the National Science Foundation, the U.S. Department of Energy and the W.M. Keck Foundation. This entire study was funded, in part, by the John Jago Trelawney Endowment to the Mineral Sciences Department of the Natural History Museum of Los Angeles County.

References

Bandy, M.C. (1938) Mineralogy of three sulfate deposits of northern Chile. *American Mineralogist*, **23**, 669–760.

Birch, W.D., Pring, A. and Wallwork, K. (2002) Mendozavilite from the Fitzgerald River District, Western Australia. *Australian Journal of Mineralogy*, **8**, 11–15.

Brown, I.D. and Altermatt, D. (1985) Bond-valence parameters from a systematic analysis of the inorganic crystal structure database. *Acta Crystallographica*, **B41**, 244–247.

Burke, E.A.J. (2008) Tidying up mineral names: an IMA-CNMNC scheme for suffixes, hyphens and diacritical marks. *Mineralogical Record*, **39**, 131–135.

Burns, P.C. and Hawthorne, F.C. (1996) Static and dynamic Jahn–Teller effects in Cu^{2+}-oxysalt minerals. *The Canadian Mineralogist*, **34**, 1089–1105.

Cook, R.B. (1978) Famous mineral localities: Chuquicamata, Chile. *Mineralogical Record*, **9**, 321–333.

Cooper, M.A. and Hawthorne, F.C. (1999) The crystal structure of betpakdalite and a new chemical formula $Mg(H_2O)_6Ca_2(H_2O)_{13}[Mo_8^{6+}As_2^{5+}Fe_3^{3+}O_{36}(OH)](H_2O)_4$. *The Canadian Mineralogist*, **37**, 61–66.

Ermilova, L.P. and Senderova, V.M. (1961) Betpakdalite – a new mineral from the oxidation zone of the Karaoba wolframite deposit. *Zapiski Vsesoyuzhogo Mineralogicheckogo Obshchestra*, **90**, 425–430, [in Russian].

Finney, J.J., Williams, S.A. and Hamilton, R.D. (1986) Obradovicite, a new complex arsenate-molybdate from Chuquicamata, Chile. *Mineralogical Magazine*, **50**, 283–284.

Gebhard, G. (1999) *Tsumeb II. A Unique Mineral Locality*. GG Publishing, Grossenseifen, Germany.

Gouzerh, P. and Che, M. (2006) From Scheele and Berzelius to Müller – polyoxometalates (POMs) revisited and the "missing link" between the bottom up and top down approaches. *L'Actualité Chimique*, **298**, 9–22.

Hatert, F., Mills, S.J., Pasero, M. and Williams, P.A. (in press) CNMNC guidelines for the use of suffixes and prefixes in mineral nomenclature, and for the preservation of historical names. *European Journal of Mineralogy*.

Holland, T.J.B. and Redfern, S.A.T. (1997) Unit cell refinement from powder diffraction data: the use of regression diagnostics. *Mineralogical Magazine*, **61**, 65–77.

Mandarino, J.A. (1981) The Gladstone–Dale relationship: Part IV. The compatibility concept and its application. *The Canadian Mineralogist*, **19**, 441–450.

Mills, S.J., Hatert, F., Nickel, E.H. and Ferraris, G. (2009) The standardisation of mineral group

hierarchies: application to recent nomenclature proposals. *European Journal of Mineralogy*, **21**, 1073–1080.

Moore, P.B. (1992) Betpakdalite unmasked, and a comment on bond valences. *Australian Journal of Chemistry*, **45**, 1335–1354.

Ossandón, C., Fréraut, R., Gustafson, L.B., Lindsay, D.D. and Zentilli, M. (2001) Geology of the Chuquicamata mine: a progress report. *Economic Geology*, **96**, 249–270.

Pope, M.T. (1983) *Inorganic Chemistry Concepts 8: Heteropoly and Isopoly oxometalates*. Springer-Verlag, Heidelberg, Germany.

Schmetzer, K., Nuber, B. and Tremmel, G. (1984) Betpakdalit aus Tsumeb, Namibia: Mineralogie, Kristallchemie und Struktur. *Neues Jahrbuch für Mineralogie, Monatshefte*, **1984**, 393–403.

Shrake, T.C., Thursten, P., Ernst, D.R. and Ashleman, J.C. (1996) Geology of Chile's Lomas Bayas porphyry copper deposit. *Mining Engineering*, **48**, 37–42.

Skvortsova, K.V., Sidorenko, G.A., Nesterova, Y.S., Arapova, G.A., Dara, A.D. and Rybakova, L.I. (1971) Sodium betpakdalite and conditions of its formation. *Zapiski Vsesoyuzhogo Mineralogicheckogo Obshchestra*, **100**, 603–611, [in Russian].

Williams, S.A. (1986) Mendozavilite and para-mendozavilite, two new minerals from Cumobabi, Sonora. *Boletín de Mineralogía*, **2**, 13–19.

Yegorov, B.L., Dara, A.D. and Senderova, V.M. (1969) Melkovite, a new phosphomolybdate from the oxidized zone. *Zapiski Vsesoyuzhogo Mineralogicheckogo Obshchestra*, **98**, 207–212, [in Russian].